Development of X-ray Sensitizer Based on Metal-Bearing Star Polymer for X-ray Sensitizing Therapy

Ahmad Kusumaatmaja

2013

Graduate School of Materials Science

Nara Institute of Science and Technology

Content

Chapter 1

General Introduction

1.1. Cancer Therapy

Cancer is one of the lethal disease in the world. Fortunately, cancer patients have many options for treatment including, surgery, chemotherapy, biologic therapies, molecular targeted therapy, stem-cell transplantations and radiotherapy[1]. The type of treatment used is based on many different factors such as the type of cancer, tumor size, malignancy, age of patient, and health of the patient. When the tumor exists as a primary tumor, surgery can be an excellent treatment option. Removal of the tumor can render a person cancer free if all the cancerous cells are removed. Quite often surgical removal of a tumor is paired with chemotherapy treatments. This helps ensure that all of the cancer cells are killed and that disease is eradicated. Chemotherapy is the use of drugs to treat the disease and usually involves the use of a combination of drugs. Combination of drug gives advantage which can act synergistically or have an additive effect. Since chemotherapeutic drugs require repeated doses in order to maximize the number of cells that are killed, therapy can last several weeks. Combination therapies can also reduce the amount of toxicity because smaller doses of each drug can be used rather than higher doses necessary for single drug therapies. The main problem with chemotherapy is toxicity due to the lack of tumor cells selectivity. Some of the more common side effects include nausea, vomiting, and fatigue. The drugs can affect many different sites throughout the body including chemoreceptors in the brain stem and gastrointestinal tract.[1] Another large problem with chemotherapy is that tumors have the ability to gain resistance to drugs. Once resistance is gained against one drug it is likely that the tumor will be resistant to any drug within the same class.

Radiation therapy is one of attracting methods to treat cancer. Radiotherapy works by damaging the DNA of cells caused by a photon, electron, proton, neutron or ion beam ionization of the atoms directly or indirectly. Radiotherapy is usually using X-ray as a light source, and is a local therapy used for the treatment of malignant tumors, which is clearly different from chemotherapy. Typical total dose for a tumor treatment ranges from 60 to 80 Gy in ca. 2 Gy each fraction, which are almost near lethal dose of the animals. Therefore, such large irradiation dose induces various adverse effects, that is an inflammation of tissues and organs in and around the body site radiated. This can cause symptoms that depend on what organs are affected and to what degree. For example, radiation therapy can inflame skin to cause a burn or permanent pigmentation, irritate the colon and cause diarrhea, and cause a decrease in the number of white blood cells, that help protect the body against infection. Although the adverse effects of radiation therapy may be unpleasant, they can usually be treated or controlled. It also helps to know that, in most cases, they are not permanent. To a great degree, the possible adverse effects of radiation therapy depend on the location and the amount of radiation dose, so that it would be helpful to develop new X-ray therapy using low irradiation dose. There are two ways to optimize radiotherapy: increase the dose absorption of radiation energy on target tumor tissue (localized energy) and inhibit the repair processes in tumor cells or tissue.[2]

1.2. Radiation

Radiation was first discovered in 1895, by Wilhelm Conrad Roentgen, and was very quickly applied medically as a treatment for various diseases. The concepts behind

the mechanism of radiation were not even fully understood at that time but only several months after its discovery radiotherapy against cancer was established. In January of 1896, Dr.Emil Grubbe, of Chicago, used radiation to treat advanced breast cancer. From that point the concept of radiotherapy became entrenched as a modality of cancer therapy. In 1913 the hot-cathode tube was invented which allowed control of the radiation dose given. The method of exposure to radiation continued to be improved after the invention of the cathode tube. The electron linear accelerator was invented in the 1940.s followed by the circular electron accelerator several years later. Both accelerators generated a higher dose of radiation to be given in a defined field. During the 1960.s the use of a radioactive implant that contained a radio-nucleotide became a common therapy allowing for short sessions outpatient of therapy. Development of assays that allowed the quantization of cell killing helped to give a better understanding of tumor cell sensitivity to radiation.

The invention of the CT scan and MRIs in the 1970.s improved the imaging of tumors. It became possible to know the exact location and size of a tumor so that better treatment plans could be made. Today it is possible to accurately deliver a beam of radiation to a tumor and even today we are still improving the efficiency and safety of this therapy.[3] Radiation therapy uses ionizing radiation to kill tumor cells which a photon, electron or proton beam will either indirectly or directly damage the DNA and when the cancer cell tries to divide, it is unable to divide and dies. It is important to know that non-cancerous cells can repair the damage caused by radiation and do not always die from its exposure. Radiation can be given to specific localized areas of the body allowing exposure to healthy cells to be minimized. One way that this is

accomplished is through lead shields, known as collimators, which reduce leakage of radiation and help target the beam to a specific area. Multi-leaf collimators are used and help to control the amount of radiation reaching healthy tissue. The use of fractionated doses of radiation also contributes to exposing only localized areas. When smaller doses of ionizing radiation are given over time rather than one large dose the amount of surrounding tissues affected is minimized.[3]

For the treatment of cancer there are two different types of radiation that can be used, external radiation therapy and internal radiation therapy. External radiation involves a beam of radiation that is directed from outside the body. X-rays and gamma rays are focused into a beam through collimators so that the tumor receives the majority of the radiation. High energy X-rays are used to treat tumors found deep in the body while electrons are used to treat superficial tumors. For internal radiation therapy (brachytherapy) the source of radiation is present within the body. The radiation source is implanted into the body either next to or directly into the tumor. Radioactive materials are used for this type of radiation therapy and include cesium, gold, and iridium. The effects that the radioactive material has on surrounding tissue are minimal.[4] The type of radiation therapy used varies based on the type of cancer, location of the tumor and the patient medical history but both have proven to be successful.[3] The similar method with brachytherapy but noninvasive is utilizing heavy metal atom to enhanced radiotherapy (metal radiosensitizer). By combining heavy metal atom with X-ray, the absorption of X-ray will increase moreover the radiotherapy efficiency is increased.

1.3. Heavy Metal Atom as X-ray Sensitizer

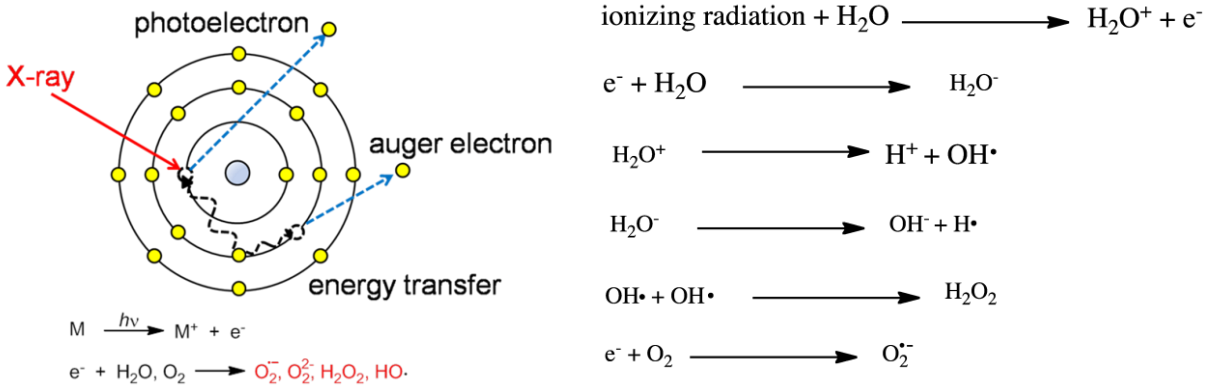

Figure 1.1. Photoelectron and auger electrons induced by X-ray irradiation

Photoelectron and auger electron are supposed to be responsible for enhancing the dose of radiation in the local area of cancer cells (**Figure 1.1**). The electron induced by X-ray irradiation reacted with the water and produced radicals that induces death of the cancer cells. **Figure 1.1** also shows the reaction between water and X-ray irradiation. Based on that knowledge, low irradiation dose of X-ray could kill the cancer if an appropriate compound (X-ray sensitizer) was combined with X-ray. X-ray photoabsorption not only produces photoelectrons, but it also induces Auger effects (and Auger electrons) at the photoabsorption site. The presence of high-Z elements produces enhanced radiobiological effects as efficiently as high linear energy transfer (LET) radiation with X-ray photon irradiation.[2]

Heavy metal atoms are chosen as candidates of X-ray sensitizer because the absorption efficiency increases roughly in proportion to Z^4-Z^5 (**Table 1.1**). Heavy metals are thought to be good X-ray sensitizer but most of them also have serious toxicity. Metal-enhanced radiation therapy had been reported by using gold

microspheres and gold nanoparticles.[2,5] These results suggested that by adding metal into the tumor cells the X-ray absorption may increase and release more electron into the solution which will interact with water to produce radicals.[6]

Table 1.1. X-ray absorption efficiency (normalized to Fe =1)

Elements	Atomic number	X-ray absorption efficiency $\sim Z^5$	Characteristic X-ray energy (keV)
P	15	*0.06*	2.01
Ca	20	*0.27*	3.69
Fe	26	*1*	6.40
Ru	44	*14*	19.27
Eu	63	*83*	41.54
W	74	*187*	59.32
Pt	78	*243*	66.83

In 2007, Takahashi et. al. reported potential radiosensitizing materials for X-ray-induced photodynamic therapy.[7] They reported that reactive oxygen species (ROS) can be generated under X-ray irradiation from TiO_2, ZnS:Ag, CeF_3 and CdSe quantum dots. The particle size of ZnS:Ag and CeF_3 were much larger than 100 nm and TiO2, CdSe quantum dots were less than 100 nm. In vitro experiment using CdSe quantum dots gave best result compare to the others sensitizing materials. Although CdSe quantum dots cannot penetrate into HeLa cells, CdSe quantum dots (about 20 nm) had sensitized the cell externally by imposing oxidative-stress or disturbing signaling

pathway triggered by receptors on the cell membrane.[7,8]

Some researchers reported that Pt and Au nanoparticles gave radiobiological enhancement when incorporated with plasmid DNA. However, it still needs modification to utilize Pt and Au nanoparticles as radiosensitizer because the Pt is very toxic and the clearance of nanoparticles from the body is slower than some small molecules, leading to longer-term whole-body retention in some cases.[2,5]

1.4. Living Radical Polymerization

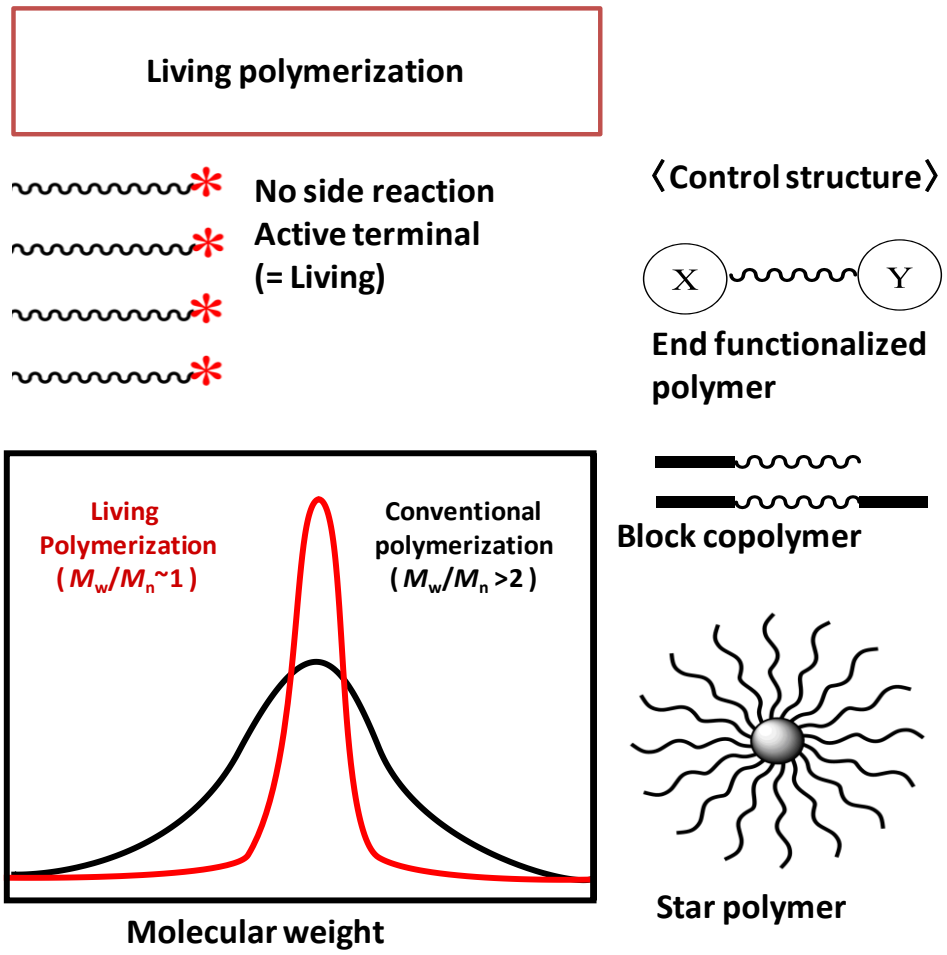

Figure 1.2. The advantages of living radical polymerization

Living radical polymerization (LRP) can be used to create polymers with precise molecular weights and tailored architectures. It can be used for the preparation of copolymers, incorporating a broad spectrum of radically (co)polymerizable monomers forming materials with predetermined molecular weight, and narrow molecular weight distribution[10] (**Figure 1.2**). The three most commonly used LRP techniques are nitroxide-mediated polymerization (NMP), atom transfer radical polymerization (ATRP), and reversible addition/fragmentation chain transfer polymerization (RAFT).[10] Recent advances in each of the LRP techniques have continued to increase the diversity of resulting polymers.

Through appropriate selection of the functional (macro)initiator, copolymers formed in a controlled/"living" polymerization process can have essentially any desired topology. Further, as noted at the foot of the figure showing what LRP can do, highlight of that mechanistic transformations permit the use of macroinitiators or macromonomers prepared by other polymerization procedures in many LRP processes which allows incorporation of a spectrum of functionalities and polymer segments prepared by any other controlled polymerization process into segments of copolymers prepared by LRP.

Numerous examples of gradient,[11] block[12] and graft[13] copolymers have been reported, as well as polymers with complex architectures, including comb shaped polymer brushes,[14] stars,[15] and hyperbranched[16] copolymers. In this research LRP is useful to construct a drug delivery which could bring and introduce metal into the tumor tissue.

1.4. Metal-Bearing Star Polymer

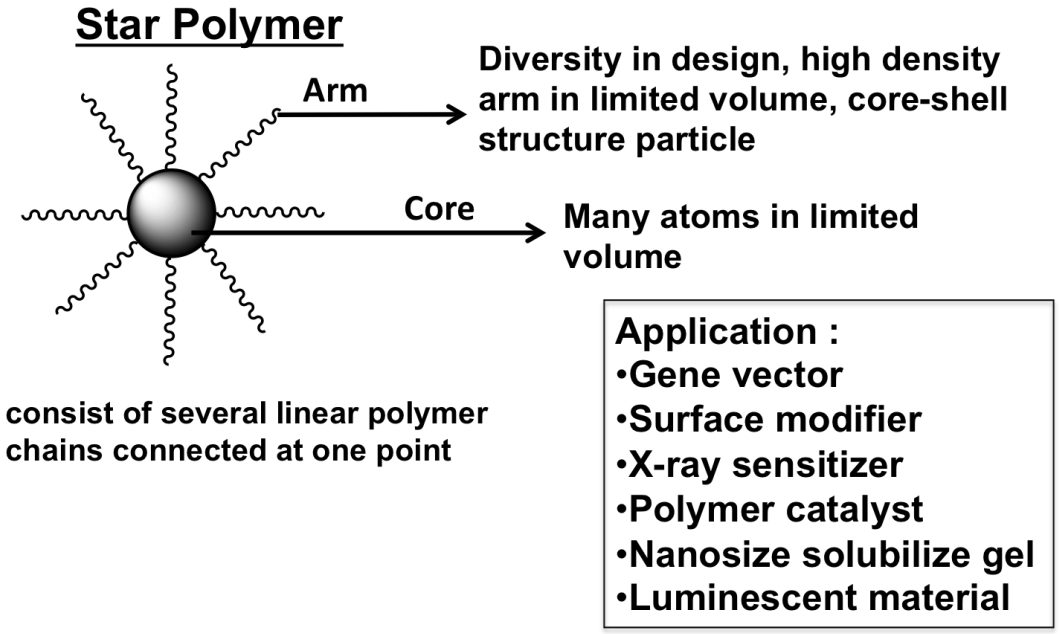

Figure 1.3. Star polymer design

To deliver heavy metal atom into the tumor tissue, drug delivery is needed. Polymers are potential to be used as drug delivery especially star polymers. Star polymers consist of several linear polymer chains connected at one point and, so it has diversity in design and high-density arm in limited volume. Changing the arm polymer could modify the properties of the star polymer which possible to be applied as gene vector, surface modifier, polymer catalyst, nanosize solubilize gel, luminescent material and also X-ray sensitizer. **Figure 1.3.** shows the advantages of the star polymer design. Star polymer was successfully synthesized since the invention of metal catalyst for controlling LRP.[17-23] Furthermore in 2001, Sawamoto and coworkers employed LRP with Ru-based initiating systems for star polymer synthesis.[24] The synthesis was

directed to star-shaped poly(methyl methacrylate) with relatively large number of arms which had controlled molecular weights and narrow molecular weight distributions (MWDs). Microgel core-functionalized star-shaped polymers were synthesized by the polymer linking reaction method in $RuCl_2(PPh_3)_3$-catalyzed LRP. Recently after Baek et. al. developed microgel star polymer, Terashima et al. in 2006 encapsulated metal catalyst into star polymer core during metal-catalyzed LRP.[25,26]

They promoted metal containing star polymer as polymer catalyst using several kind of metals (Ru, Ni and Fe).[27] The metals were encapsulated in the core of star polymer by using phosphine ligand. The key is copolymerizing a phosphine-carrying monomer (*p*-styryldiphenyl phosphine) that can serve as a ligand for the metals (Ruthenium) *via* ligand exchange in the linking reaction of linear polymers with a divinyl compound. Polyethylene glycol (PEG)-armed star polymers had also been developed which were found to be amphiphilic. [28]

1.5. Europium (Eu(III))

Eu(III) is chosen as candidate for X-ray sensitizer because its high atomic number and luminescence properties. Combination of high absorption of X-ray and luminescence properties of Eu(III) are considered to be applied for curing and detecting tumour tissues. The photophysical properties of Eu(III) ions are perhaps the most studied of all of the lanthanide ions. Since both of the levels involved in the luminescent transition are nondegenerate, only one emission line is observed at near 580 nm when a single chemical species is present.[28,29,30] As shown in **Figure 1.4**, the lowest energy emissive state, $^5D_0$, is 17,250 cm^{-1} above the $^7F_0$ ground state. In coordinating

solvents the emission of the Eu(III) ion is quenched by OH, NH and CH groups at or near the coordination site, and it has been shown that this quenching can be reduced by deuterium substitution.[31-33] The number of coordinated OH groups from water or methanol can be estimated from changes in the lifetime by the Horrocks equation, although this relation is not very accurate when the number of OH groups in the first coordination sphere is small.[34] Encapsulation of the ion by various chelators can increase the emission quantum yield of a complex compared to the free ion. For example, the complex $Eu(TTA)_3 \cdot 2DMSO$ (TTA = thenoyl trifluoroacetonate) in DMSO showed Eu(III) based emission with a lifetime of 0.72 ms, whereas the hydrated complex exhibits only weak emission from the ligand triplet state.[35]

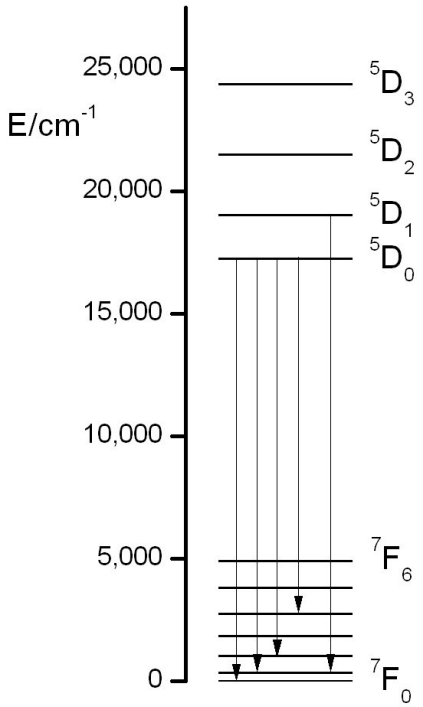

Figure 1.4. Energy levels of Eu(III) ions

1.7. Aims of the Research

As described above, the developments of new method for cancer therapy have been most attractive in this field, because the noninvasive cancer treatment using metal enhanced radiotherapy is very promising now. In this research, I chose Europium(III) atom as the candidate of radiosensitizer because of its high *Z* number (63) and also the K-shell absorption edge of Eu atom is relatively close to the characteristic X-ray energy emitted from tungsten(W) as common target on the X-ray generator. Furthermore, the toxicity of Eu(III) is relatively lower than that of other heavy metal atom. The luminescence properties of Eu(III) is also the advantages, because from those properties, Eu(III)-bearing star polymer could be employed not only for curing the cancer cells but also to imaging the cancer tissues. In this research, I focused on the syntheses of Eu(III)-bearing star polymer (optimizing the concentration of Eu(III) and also obtaining the water-soluble Eu(III)-bearing star polymers) and increasing the dose of radiation in certain place (local dose enhancement in the cancer area) by using specific material that can absorb X-ray radiation therefore low irradiation dose of X-ray could be used. In general, the aim of this research is to develop X-ray sensitizer based on metal-bearing star polymer.

In this study, the X-ray sensitizer (Eu-star polymer) was synthesized by LRP. Eu atom was introduced into the core of star polymer using a ligand monomer (styryldiphenyl phosphine oxide-SDPO) that can serve as ligand for Eu atom. In chapter 2, the synthesis and the photoproperties were explained in detail. Eu-star polymer as X-ray sensitizer will be activated by X-ray irradiation to generate radicals inside or outside

the targeted cancer cell and induce cell death by causing functional disorder. In chapter 3 the X-ray sensitizing experiment using plasmid DNA was presented to confirm the dose enhancement of Eu-star polymer. Eu-star polymer as X-ray sensitizer was supposed to penetrate inside or outside of cancer cells. The concept of Enhanced Permeability and Retention (EPR) also supported the idea for delivering drug sensitizers (Eu(III)-bearing star polymer) into the cancer tissues.[36]

1.9. References

1. Tannock, I.F., Hill, R.P., Bristow, R.G., Harrington, L. The Basic Science of Oncology, Fourth Edition. Toronto; McGraw-Hill, 2005.

2. Kobayashi, K; Usami, N; Porcel, E; Lacombe, S and Le Sech, C. *Mutat. Res.* **2010**, *704*, 123-131.

3. Bernier, J.; Hall, E.J.; Giaccia, A. *Nature*, **2004,** *4*, 737-747.

4. Washington, C. M.; Leaver, D. Principles and practice of Radiation Therapy, Second Edition. St. Louis; Mosby, 2004.

5. Hainfeld, JF; Dilmanian, A; Slatkin DN and Smilowitz, HM. *J. Pharm. Pharmacol.* **2008**, *60*, 977-985.

6. Herold, D.; Das, I.; Stobbe, C.; Iyer, R.; Chapman. *Int. J. Radiat. Biol.* **2000**, *76*, 1357.

7. Takahashi, J; Misawa M. *Nanobiotechnol* **2007**, *3*, 116-126.

8. Carter, JD.; Cheng, NN.; Qu, Y.; Suarez, GD.; Guo, T. *J. Phys. Chem. B* **2007**, *111*, 11622-11625.

9. von Sonntag, C. *The Chemical Basis for radiation Biology*, Taylor and Francais; London, 1987.

10. Matyjaszewski, K.; Xia, *J. Chem. Rev.* **2001**, *101*, 2921-2990.

11. Listak, J.; Jakubowski, W.; Mueller, L.; Plichta, A.; Matyjaszewski, K.; Bockstaller, M. R. *Macromolecules* **2008**, *41*, 5919-5927.

12. Matyjaszewski, K. *Macromol. Symp.* **1996**, *111*, 47-61.

13. Matyjaszewski, K. Cationic Polymerizations: Mechanisms, Synthesis, and Applications.*;* Dekker: New York, 1996.

14. Matyjaszewski, K.; Ziegler, M. J.; Arehart, S. V.; Greszta, D.; Pakula, T. *J. Phys. Org. Chem.* **2000**, *13*, 775-786.

15. Davis, K. A.; Matyjaszewski, K. *Advances in Polymer Science* **2002**, *159*, 2-166.

16. Gaynor, S. G.; Matyjaszewski, K. *ACS Symp. Ser.* **1998**, *685*, 396.

17. Beers, K. L.; Gaynor, S. G.; Matyjaszewski, K.; Sheiko, S. S.; Moeller, M. *Macromolecules* **1998**, *31*, 9413-9415.

18. Kato, M; Kamigaito, M; Sawamoto, M. *Macromolecules* **1995**, *28*, 1721.

19. Ando, T; Kato, M; Kamigaito, M; Sawamoto, M. *Macromolecules* **1996**, *29*, 1070.

20. Ando, T; Kamigaito, M; Sawamoto, M. *Macromolecules* **1998**, 31, 6708.

21. Takahashi, H; Ando, T; Kamigaito, M; Sawamoto, M. *Macromolecules* **1999**, *32*, 3820.

22. Ando, T; Kamigaito, M; Sawamoto, M. *Macromolecules* **2000**, *33*, 5825.

23. Ando, T; Kamigaito, M; Sawamoto, M. *Macromolecules* **2000**, *33*, 2819.

24. Ando, T; Kamigaito, M; Sawamoto, M. *Macromolecules* **2000**, *33*, 6732.

25. Baek, K-Y; Kamigaito, M; Sawamoto, M. *Macromolecules* **2001**, *34*, 215.

26. Terashima, T; Kamigaito, M; Baek, K-Y; Ando, T; Sawamoto, M. *J. Am. Chem. Soc.* **2003**, *125*, 5288.

27. Terashima, T; Ouchi, M; Ando, T; Kamigaito, M; Sawamoto, M. *Macromolecules* **2007**, *40*, 3581.

28. Terashima, T.; Nomura, A.; Ito, M.; Ouchi, M.; Sawamoto, M. *Angew. Chem. Int. Ed.* **2011**, 50, 7892.

29. Horrocks, Jr. W. D.; Albin, M. *Prog. Inorg. Chem.* **1984**, *31*, 1

30. Bünzli, J.-C. G.; Choppin, C.R. Lanthanide Probes in Life, Chemical and Earth Sciences, Chapter 1, Elsevier, Amsterdam, 1989.

31. Buono-Core, G. E.; Li, H,; Marciniak, B. *Coord. Chem. Rev*. **1990,** *99*, 55.

32. Oude Wolbers, M. P.; van Veggel, F. C. J. M.; Snellink-Ruël, B. H. M.; Hofstraat, J. W.; Geurts, F. A. J.; Reinhoudt, D. M. *J. Am. Chem.Soc.* **1997**, *119*, 138.

33. Hemmilä, I.; Mukkala, V.-M.; Takalo, H. J. *Fluorescence*, **1995**, *5*, 159.

34. Dickins, R.S.; Parke, D.; de Sousa, A. S.; Williams, J. A. G. *Chem.Commun.* **1996**, 697.

35. Horrocks, Jr. W.D.; Sudnick, D. R. *Acc. Chem. Res.* **1981**, *14*, 384

36. Brito, H. F.; Malta, O. L.; Menezes, J. F. S. *J. Alloy Cmpds.* **2000**, *336,* 303-304.

37. Matsumura, Y.; Maeda, H. *Cancer Res.* **1986**, *46*: 6387-6392.

Chapter 2

Synthesis and Photoproperties of Eu(III)-bearing Star Polymers as Luminescent Materials

2.1. INTRODUCTION

The construction of various functional polymers has been studied in recent years. Furthermore, control of polymer size, monomer sequences, number and position of functional groups, and polymer architecture are still state-of-the-art materials science issues.[1–3] One of the targets of functional polymers is an area of biorelated polymers in which drug or gene delivery,[4] materials for medical devices,[5] and bioimaging probes[6] are applied. Many polymers have been reported as bioimaging probes, some of which have organic luminescent dyes such as Rhodamine[7–9] and coumarin[10,11] in their side chain or terminal. Organic luminescent dyes especially fluorescein, however, have several drawbacks, being easily photobleached and decomposed because of poor photochemical stability.[12] Lanthanide(III) complex-based luminescent dyes have been attracting attention as alternatives to organic luminescent dyes in recent years. Lanthanide(III)-based luminescent materials generally have high photochemical stability in both the ground and excited states and the long lifetime of the excited states allows the use of time-resolved detection, a definite asset for bioassays and luminescent microscopy.[13–15] Considering the biological applications, lanthanide(III)-based luminescent materials should be water-soluble. There have been some attempts to

obtain water-soluble lanthanide(III) luminescent materials by complexation of lanthanide(III) (europium (Eu), terbium(Tb)) with pyridine-2,4,6-tricarboxylic acid (H_3PTA)[13] or incorporation into nanoparticles.[16–19] Water-soluble Eu(III) and Tb(III) complexes have been reported as binding tags for studying protein interactions,[20,21] or bacterial spore[22] or singlet oxygen[23] detection, for signaling of carbonate chelation,[24] as labels for prolactin in human serum,[25] and as luminescent tags on magnetic nanoparticles for cell imaging applications.[26] However, it is known that Eu(III) complexes are unstable in aqueous medium[27] and thus there are few water-soluble polymers that have lanthanide ions in the side chain. Multidentate ligands are required to stabilize lanthanide ions in water and there are some complicated synthetic chemistries to obtain such lanthanide-stabilizing monomers. It is equally important to note that the multidentate group-containing monomer may cause side reactions via interaction with polymerization catalysts or propagating species.

Living radical polymerization (LRP) has been applied for syntheses of various functional polymeric materials in recent years because the growing species (radicals) are stable for many types of functional groups. Various metal-conjugating polymers have been prepared by LRP.[28,29] Copolymerization of divinyl monomer and ligand

monomer, which can coordinate to a polymerization metal catalyst, from living polymer (macroinitiator) leads to a star polymer bearing many metal complexes in the core in a one-pot reaction, which is a very simple method to introduce metal ions.[30–34] Interestingly, the stability of the metal complex in the core of the star polymer was higher than that of the corresponding metal complex, probably because of the chelating effect.[34] These results prompted us to investigate the introduction of lanthanide ions into a star polymer as an easy method to prepare a water-soluble and water-stable luminescent polymer. I employed poly(ethylene oxide) (PEO) as a water-solubilizing chain and a tris(hexafluoroacetylacetonato)europium(III) bis(triphenylphosphine oxide) [Eu(III)-tppo] complex derivative, which is a typical luminescent complex having a high quantum yield and is easy to prepare.[35,36] I first explored a suitable introduction method for Eu(III) ion using poly(methyl methacrylate) as a model arm polymer for star polymer formation and then prepared Eu(III)-bearing PEO star polymer. The photoproperties (quantum yield and emission lifetime) of the obtained polymers are also discussed.

2.2. EXPERIMENTAL

2.2.1. Materials

Methyl methacrylate (MMA, Tokyo Chemical Industry Co., purity > 99%), ethylene glycol dimethacrylate (EGDMA, Sigma-Aldrich, purity > 98%), and toluene (Sigma-Aldrich, purity > 99%) were purified by distillation over calcium hydride under reduced pressure before use. Poly(ethylene glycol) monomethyl ether (Sigma-Aldrich, $M_n \approx 10{,}000$ g/mol), $Ru(Ind)Cl(PPh_3)_2$ (STREM, purity > 98%), 1,1,1,5,5,5-hexafluoro-2,4-pentanedione (Sigma-Aldrich, purity > 98%), *p*-styryldiphenyl phosphine (SDP, donated by Hokko Chemical Industry Co.), and europium acetate n-hydrate (Wako Pure Chemical Industries, purity > 98%) were used as received. Chlorine-terminated poly(ethylene oxide) (PEO-Cl macroinitiator) was synthesized according to the literature.[37,38] Tris(hexafluoroacetylacetonato)europium(III) dihydrate $[Eu(hfa\text{-}H)_3(H_2O)_2]$ was prepared according to the literature.[35]

2.2.2. Instruments

Gel permeation chromatography (GPC) on three linear-type poly(2-hydroxyethyl

methacrylate) gel columns (Shodex SB-806M; exclusion limit 2×10^7; 0.8 cm i.d. × 30 cm) that were connected to a JASCO PU-2080 precision pump (Jasco Co., Ltd.), a JASCO RI-2031 refractive index detector (Jasco Co., Ltd.), and a JASCO UV-2074 UV/Vis detector (Jasco Co., Ltd.) set at 270 nm was used to determine molecular weights (M_n) and molecular weight distributions (M_w/M_n) of polymer samples with respect to poly(methyl methacrylate) (PMMA) standards. The absolute weight-average molecular weight (Mw) of the star polymers was determined by multiangle laser light scattering (MALLS) in DMF containing 10 mM LiBr at 40 °C on a Dawn E instrument (Wyatt Technology Corp., Ga-As laser, λ = 690 nm). ^{1}H, ^{13}C, and ^{31}P NMR spectra were obtained on a JEOL Ltd. JNM-ECP 500. ^{1}H and ^{13}C NMR chemical shifts were determined using tetramethylsilane (TMS) as an internal standard, whereas ^{31}P NMR chemical shifts were determined using 85% phosphoric acid as an external standard. UV-vis spectra were recorded on a JASCO V-570 spectrophotometer. Microwave-induced plasma–mass spectrometry (MIP–MS) P-6000 (Hitachi) was used to determine the Eu(III) ion concentrations in the core of the star polymer. Fluorescence spectra were recorded on an F-2500 spectrophotometer (Hitachi). Elemental analyses were performed on a PerkinElmer 2400 series II CHNS/O elemental analyzer (PerkinElmer, Inc. The emission quantum yields were

determined using an absolute PL quantum yields measurement system (Hamamatsu Photonics, C9930-02). Emission lifetimes were measured with the third harmonic (355 nm) of a Q-switched Nd-YAG laser (Spectra Physics, INDI-50, fwhm = 5 ns, λ = 1064 nm) and a photomultiplier (Hamamatsu Photonics, R5108, response time ≤ 1.1 ns). The hydrodynamic diameter of the Eu-bearing PEO star polymer was measured using a dynamic light scattering spectrometer equipped with a 633 nm He-Ne laser (Zetasizer Nano-ZS, Malvern).

2.2.3. Synthesis of *p*-styryldiphenyl phosphine oxide (SDPO)[39]

SDPO was synthesized according to the literature.[39] SDP (17.4 mmol, 5.00 g) was added to a round-bottom flask and then dissolved in 1,2-dichloroethane (100 mL). Saturated aqueous solutions of oxone (34.8 mmol, 21.4 g) and methanol (20 mL) were added to the reaction flask and the mixture was left to stir for ca. 2 h. The reaction mixture and a large excess of water were added in a separatory funnel, and the two layers were separated. The organic layer was retained and the solvent was removed in vacuum. The sticky solid was washed with cyclohexane and then filtered to obtain SDPO as a white powder (yield: 88%). The product was characterized by ^{1}H, ^{13}C, and ^{31}P NMR. ^{1}H NMR (500.17 MHz, $CDCl_3$, TMS = 0 ppm, δ ppm): 7.44–7.69 (14H, m,

Ar*H*), 6.74 (1H, dd, *J* = 17.6, 10.8 Hz, C*H*), 5.86 (1H, dd, *J* = 17.6, 0.8 Hz, CH_2), 5.38 (1H, dd, *J* = 11.2, 0.8 Hz, CH_2). ^{13}C NMR (100.40 MHz, $CDCl_3$ = 77.0 ppm, δ ppm): 141.12 (Cipso), 135.94 (s, C2), 132.98 (CipsoP), 132.51 (s, CipsoP), 132.10–132.40 (Car, meta, Cipso, Car, orthoP), 128.62 (d, Car, metaP, *J* = 12.3 Hz), 126.31 (d, Car, ortho, *J* = 12.2 Hz), 116.73 (s, C2). ^{31}P NMR (202.47 MHz, $CDCl_3$, δ ppm): 30 ppm. Anal. calcd for $C_{20}H_{17}PO$: C, 78.6; H, 5.6%. Found: C, 78.4; H, 5.6%.

2.2.4. Synthesis of tris(hexafluoroacetylacetonato)europium(III) bis(styryldiphenyl phosphine oxide) (Eu(hfa-H)$_3$(SDPO)$_2$)

Methanol (25 mL) containing Eu(hfa-H)$_3$(H_2O)$_2$ (1.00 g, 1.25 mmol) and SDPO (0.76 g, 2.50 mmol) was stirred for 24 h in a dry round-bottom flask. The reaction mixture was concentrated using a rotary evaporator and the product was precipitated by addition of excess hexane (yield: 80%). The product was characterized by ^{1}H and ^{31}P NMR. ^{1}H NMR (500.17 MHz, $CDCl_3$, TMS= 0 ppm, δ ppm): 7.60–9.00 (28H, m, Ar*H*), 6.85 (2H, dd, *J* = 17.6, 10.8 Hz, 2-C*H*), 5.91 (2H, dd, *J* = 17.6, 0.8 Hz, CH_2,), 5.65 (3H, s, CH_3), 5.40 (2H, dd, *J* = 11.2, 0.8 Hz, CH_2,). ^{31}P NMR (202.47 MHz, $CDCl_3$, δ ppm): 29.00 ppm. Anal. calcd for $C_{55}H_{37}O_8F_{18}P_2Eu$: C, 47.81; H, 2.70%. Found: C, 47.58; H, 2.87%.

2.2.5. Synthesis of Eu(III)-bearing PMMA star polymer (Eu-PMMA star)

The polymerization was carried out using a syringe technique under argon in a flask equipped with a three-way stopcock. The reaction solution was prepared by adding sequentially in the order: $Ru(Ind)Cl(PPh_3)_2$ (0.20 mmol, 172 mg), toluene (26 mL) and MMA (200 mmol, 21.4 mL), *n*-Bu_3N (2.00 mmol, 2.00 mL, 1.0 M in toluene), and ECPA (2.00 mmol, 0.34 mL). The total volume of the reaction mixture was thus 50 mL. The flask was then placed in an oil bath at 80 °C. Samplings were done in a predetermined period to estimate the conversion. The reaction was terminated by cooling in an ice bath. The obtained PMMA was purified by silica gel column chromatography (using toluene as an eluent) and precipitated in hexane. The pure PMMA was characterized by GPC ($M_n \approx 10{,}700$; $M_w/M_n = 1.3$).

Two methods were employed for introducing Eu(III) ions into the PMMA star polymer: sequential and simultaneous introduction. For the sequential introduction method (**Scheme 2.1A**), PMMA star was synthesized by adding EGDMA (0.84 mmol, 0.84 mL, 1.0 M in toluene), SDPO (0.42 mmol, 0.42 mL, 1.0 M in toluene), *n*-Bu_3N (0.17 mmol, 0.15 mL, 1.130 M in toluene), and $Ru(Ind)Cl(PPh_3)_2$ (8.4 μmol, 7.3 mg) into the solution of PMMA (0.084 mmol, 1.0 g) in toluene (4.52 mL). The final mole ratio was

PMMA/EGDMA/SDPO/Ru(Ind)Cl(PPh_3)$_2$/*n*-Bu_3N = 13.3/133/66.5/1.33/26.6. The mixture was placed in an oil bath at 80 °C. PMMA star formation was observed by GPC analysis. The reaction was terminated by cooling in an ice bath. The product was then purified by silica gel column chromatography using toluene as an eluent (for removing the remaining Ru catalyst) and precipitated in hexane (yield: 94%, from the GPC curve area). The Eu(III) ion was introduced into the core of the PMMA star by the following technique. In a glass flask with a three-way stopcock under argon gas, PMMA star (with phosphine oxide amount = 18.2 μmol, 100 mg) and Eu(hfa-H)$_3$(H_2O)$_2$ (9.1 μmol, 7.4 mg) was dissolved in mixed solvent (2 mL, toluene:EtOH = 1:1, v/v). The solution was placed in an oil bath at 70 °C for 24 h. After cooling to room temperature, the mixture was precipitated in methanol to recover Eu-PMMA star polymer.

For the simultaneous introduction method (**Scheme 2.1B**), PMMA star polymer was synthesized by adding EGDMA (0.40 mmol, 0.40 mL, 1.0 M in toluene), Eu(hfa-H)$_3$(SDPO)$_2$ (0.10 mmol, 0.14 g), *n*-Bu_3N (0.080 mmol, 0.10 mL, 710 mM in toluene), and Ru(Ind)Cl(PPh_3)$_2$ (4.0 μmol, 3.4 mg) to the solution of PMMA in toluene (2.5 mL). The final mole ratio was

PMMA/EGDMA/Eu(hfa-H)$_3$(SDPO)$_2$/Ru(Ind)Cl(PPh$_3$)$_2$/*n*-Bu$_3$N = 13.3/133/33.3/1.33/26.6. The solution was placed in an oil bath at 80 °C. Eu-PMMA star formation was observed by GPC analysis. The reaction was terminated by cooling in an ice bath. The product was purified by silica gel column chromatography using toluene as an eluent and precipitated in methanol (yield: 92%, from GPC curve area). The introduction of core-bound Eu(III) ion was characterized by UV-vis spectroscopy and MIP–MS.

2.2.6. Synthesis of Eu(III)-bearing PEO star polymer (Eu-PEO star)

Eu-PEO star polymer was synthesized by adding EGDMA (0.075 mmol, 0.075 mL, 1.0 M in toluene), Eu(hfa-H)$_3$(SDPO)$_2$ (0.075 mmol, 104 mg), *n*-Bu$_3$N (0.060 mmol, 0.085 mL, 710 mM in toluene), and Ru(Ind)Cl(PPh$_3$)$_2$ (1.3 μmol, 2.6 mg) to a solution of PEO-Cl macroinitiator ($M_n \approx$ 10,000 g/mol, 0.030 mmol, 300 mg) in toluene (2.1 mL) using the simultaneous introduction method. The final mole ratio was thus PEO-Cl/EGDMA/Eu(hfa-H)$_3$(SDPO)$_2$/Ru(Ind)Cl(PPh$_3$)$_2$/*n*-Bu$_3$N = 13.3/33.3/33.3/1.33/26.6. Immediately after mixing, the mixture was placed in an oil bath at 80 °C. Eu-PEO star formation was observed by GPC analysis. The reaction was terminated by cooling in an ice bath. The product was then purified by silica gel

column chromatography and precipitated in cold ether. The Eu(III) ion concentration was determined by UV-vis spectroscopy and MIP–MS.

2.3. Results and Discussion

2.3.1. Synthesis of Eu-PMMA star: investigation of Eu(III) ion introduction

Introduction of Eu(III) ions into the core of the star polymer was first investigated using chlorine-terminated living PMMA as a model arm polymer. Two introduction strategies were examined. First, ligand groups and Eu(III) ions were sequentially introduced in this order (sequential introduction in **Scheme 2.1A**) because the Eu(III) center may affect polymerization catalyst for star polymer synthesis. EGDMA as a linking agent and SDPO as a ligand monomer for Eu(III) core were copolymerized from a PMMA macroinitiator coupled with $Ru(Ind)Cl(PPh_3)_2$ and *n*-Bu_3N in toluene at 80 °C to form the ligand-bearing star polymer with final molar ratio of used compounds PMMA/EGDMA/ SDPO/$Ru(Ind)Cl(PPh_3)_2$/*n*-Bu_3N = 1/10/5/0.1/2. After 48 h, the PMMA arm, EGDMA, and SDPO were successfully consumed to give a ligand-bearing PMMA star in high yield (94% calculated from the area under the GPC curve) (**Fig. 2.1a**).

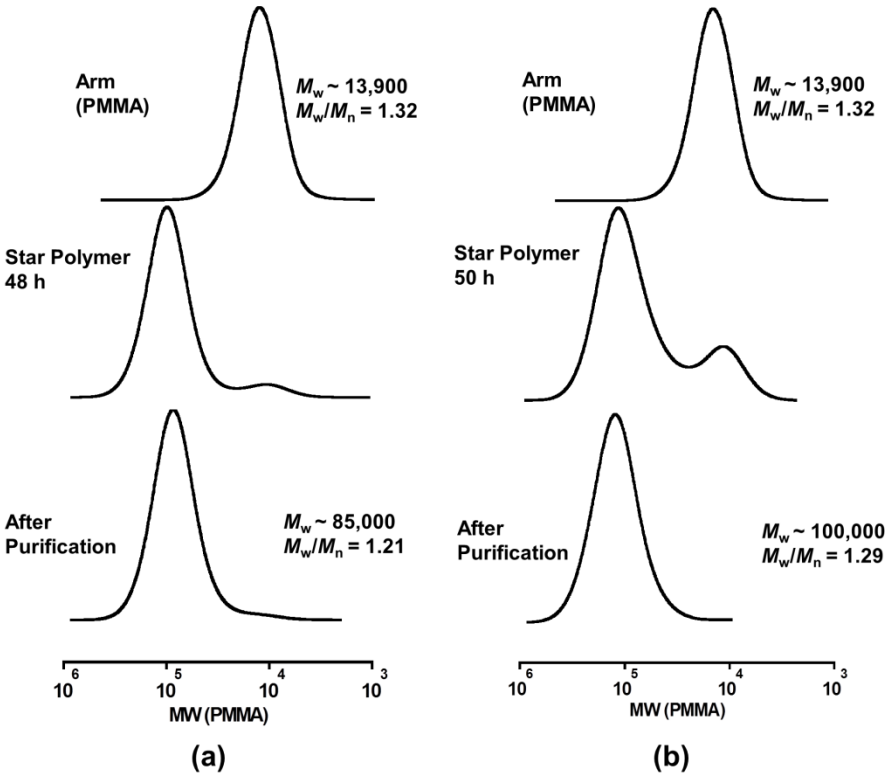

FIGURE 2.1 MWD curves of Eu-PMMA star obtained from PMMA arms by (a) sequential introduction with EGDMA and Eu(SDPO) in toluene at 80 °C: $[PMMA]_0$ = 13.3 mM; $[EGDMA]_0$ = 133 mM; $[SDPO]_0$ = 66.5 mM; $[Ru(Ind)Cl(PPh_3)_2]_0$ = 1.33 mM; $[n\text{-}Bu_3N]_0$ = 26.6 mM and (b) simultaneous introduction obtained from PMMA arms with EGDMA and Eu(SDPO) in toluene at 80 °C: $[PMMA]_0$ = 13.3 mM; $[EGDMA]_0$ = 133 mM; $[Eu(SDPO)]_0$ = 33.3 mM; $[Ru(Ind)Cl(PPh_3)_2]_0$ = 1.33 mM; $[n\text{-}Bu_3N]_0$ = 26.6 mM.

The unreacted PMMA arm and Ru catalyst were removed by precipitation with toluene/methanol and silica gel column chromatography with toluene as an eluent. The ligand-bearing PMMA star polymer was then mixed with $Eu(hfa\text{-}H)_3(H_2O)_2$ in

toluene/methanol to introduce Eu(III) ions into the core. The Eu-PMMA star had a high molecular weight (M_w = 340,000 from GPC-MALLS) and relatively narrow molecular weight distribution (MWD; M_w/M_n = 1.21 from GPC) (Table 2.1). By comparison with M_w of the PMMA arm and using the literature method,[29,30,37] the number of arms on the star was calculated as ca. 18 (**Table 2.1**).

TABLE 2.1 Eu(III)-bearing star polymers with different arm polymers

Arm	$M_{w,arm}$ (GPC)	$M_{w,star}$ (GPC)	$M_w/M_{n,star}$ (GPC)	$M_{w,star}$ (MALLS)	f [a] (No. of Arms)	[Eu(III)] (μmol/g-polymer)	
PMMA (sequential)	13,900	85,000	1.21	340,000	18	0.33[b]	1.78[c]
PMMA (simultaneous)	13,900	100,000	1.29	210,000	11	26[b]	28[c]
PEO	12,300	125,000	1.58	96,000	7	33[b]	39[c]

[a] Mole fraction of arm monomer × $M_{w,star}$(MALLS)/$M_{w,arm}$.

[b] Determined by UV-vis spectroscopy.

[c] Determined by MIP–MS.

As a second method, the Eu(III)-bound ligand monomer [Eu(SDPO)] was introduced in one step (simultaneous introduction in Scheme 2.1B). Eu(SDPO) was prepared separately and used for the star polymer formation in conjunction with EGDMA. The

star polymer formation proceeded successfully to give the Eu-PMMA star in high yield (ca. 88%), which was similar to that of the sequential introduction procedure (Fig. 1b), which suggested that the Eu(III) core shows no crucial inhibition of the catalytic activity of the Ru complex.

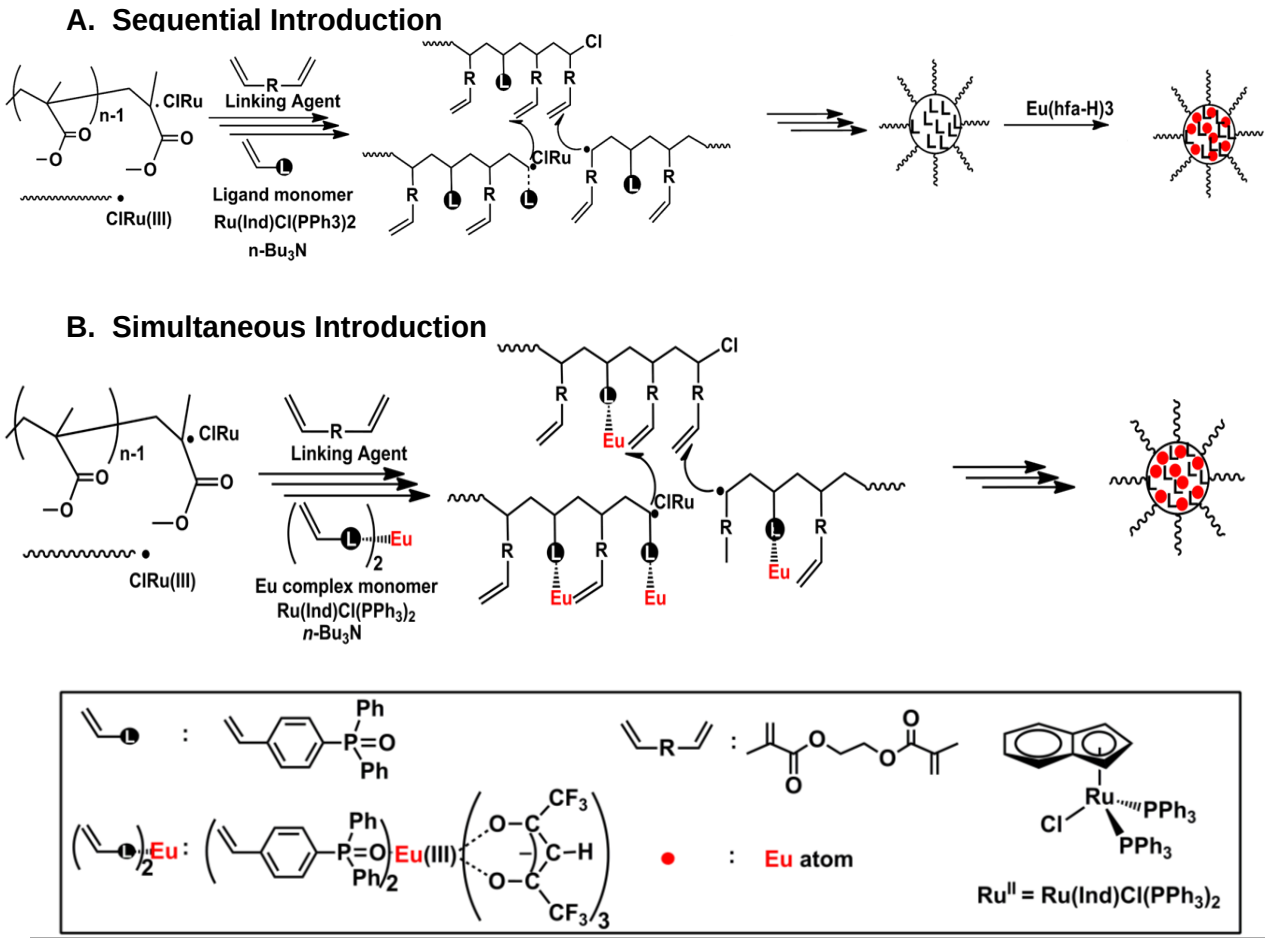

SCHEME 2.1 Syntheses of Eu(III)-bearing star polymer by living radical polymerization: sequential (**A**) and simultaneous (**B**) introduction.

The obtained PMMA star polymer had ca. 11 arms and its MWD was relatively narrow

(M_w/M_n = 1.29 from GPC). The number of arms was a little smaller than that prepared by the sequential introduction procedure, which might be due to some weak interaction between the Eu(SDPO) with the Ru complex or a difference of the core structure of the star polymers because Eu(SDPO) would work as a bifunctional monomer whereas SDPO works as a monofunctional monomer.

Quantification of the introduced Eu(III) ions: effect of introduction procedures

The amount of introduced Eu(III) ion was quantified by means of UV absorption[30] and the MIP–MS technique. The Eu(SDPO) complex and the Eu(III)-bearing star polymers have λ_{max} at 305 nm in the UV-vis spectra while the ligand monomer SDPO showed no absorbance (**Figure 2.2**). The concentration of Eu(SDPO) complex was calibrated by the absorption at 305 nm (**Figure 2.3**). UV-vis spectra of the obtained Eu-PMMA star using the sequential and simultaneous methods were very close to that of the Eu(SDPO) complex and the concentrations were estimated according to the calibration. The amounts of Eu(III) in the core of the star polymers obtained via the sequential and simultaneous methods were 0.33 and 26 μmol/g-polymer, respectively (**Table 2.1**). The amount of Eu(III) ions using the simultaneous introduction procedure was ca. 80 times larger than that using the sequential introduction procedure. The

difference may arise from the phosphine oxide groups being located in a three-dimensionally random manner in the core in the star polymer formation for sequential introduction and the ratio of two phosphine oxide groups that can coordinate to Eu(III) ion was very low, whereas the phosphine oxide groups had already coordinated and they were located at the appropriate position in the star polymer formation by simultaneous introduction. The concentration of Eu(III) ions estimated from UV absorption for the star polymer prepared by the simultaneous procedure was very close to that determined by MIP–MS. However, the concentration of Eu(III) by the sequential method estimated from UV absorption was much lower (0.33 μmol/g-polymer) than that measured by MIP–MS (1.78 μmol/g-polymer). This result is probably due to coordination not only to the triphenylphosphine oxide ligand but also to the carbonyl group in the PMMA side chain in the case of sequential introduction. From these results, the simultaneous introduction procedure is judged to be superior to the sequential introduction procedure.

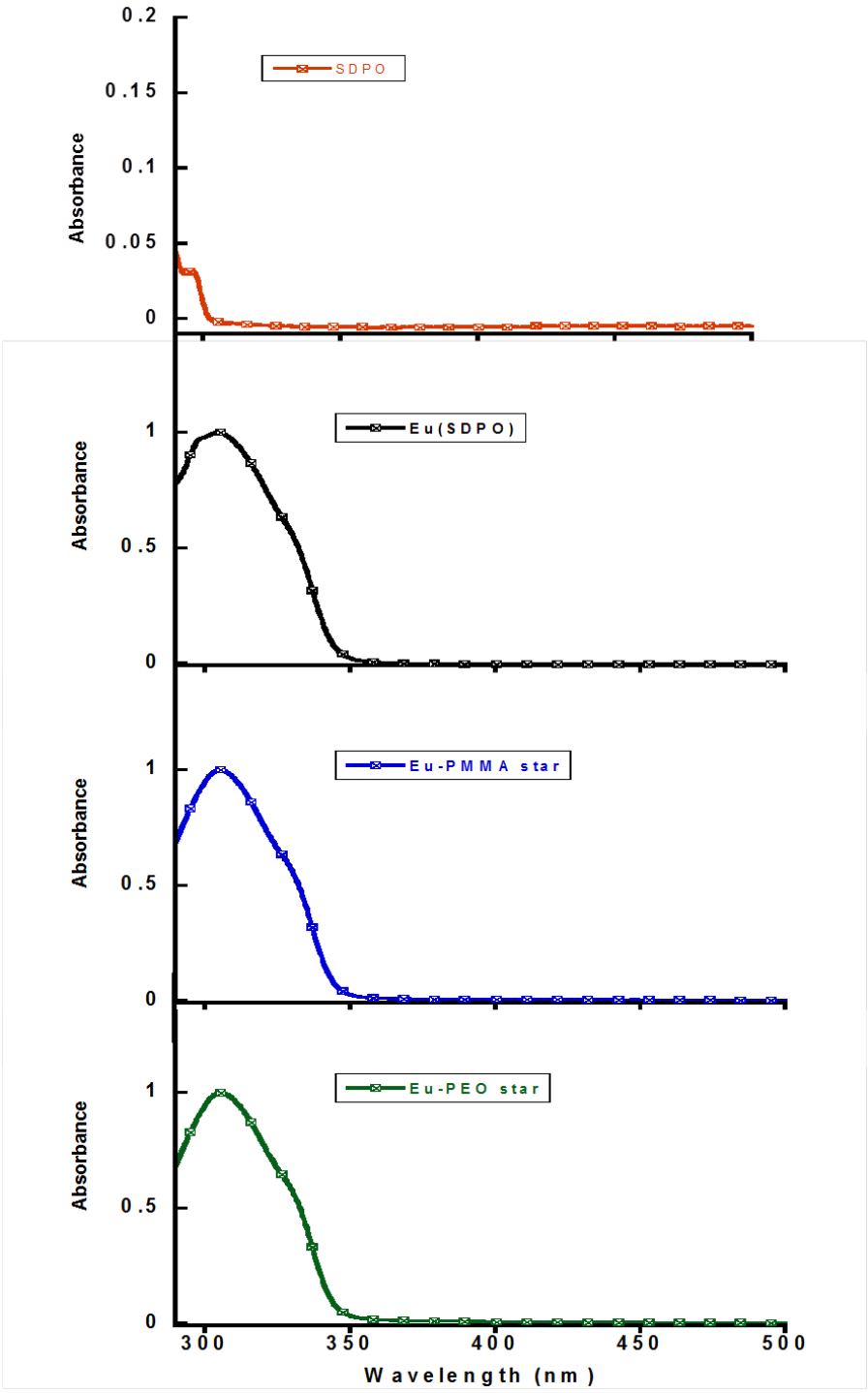

FIGURE 2.2. UV-vis spectra of SDPO, Eu(SDPO), Eu-PMMA star, and Eu-PEO star in CH_2Cl_2.

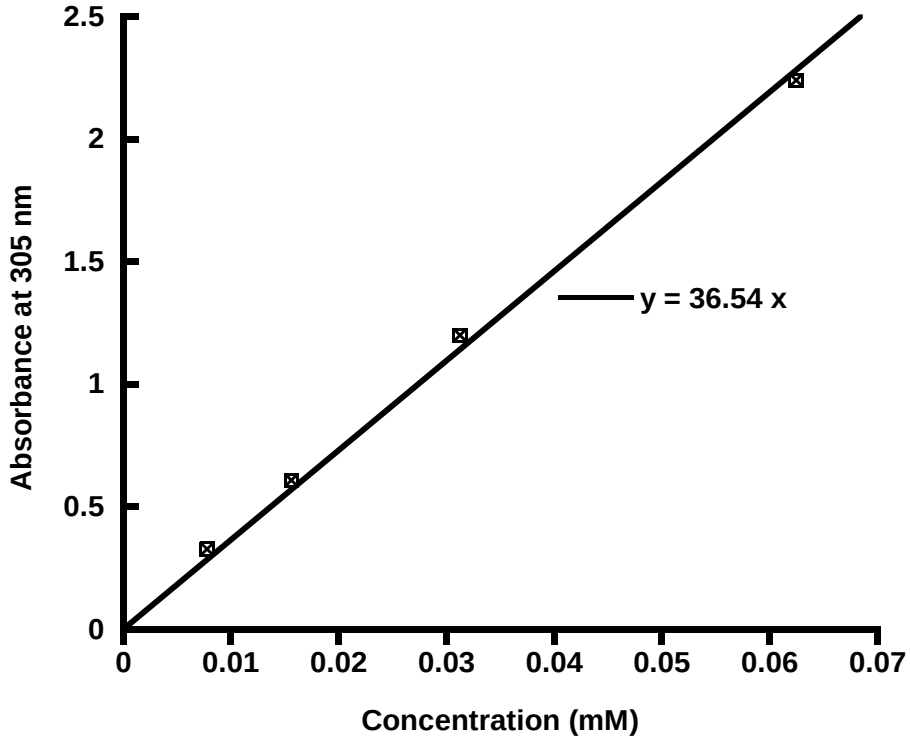

FIGURE 2.3. Calibration plot of Eu(SDPO) from the absorption of Eu(SDPO) at 305 nm at different concentrations.

Synthesis of Eu-PEO star

Synthesis of water-soluble Eu(III)-bearing star polymer was then examined. PEO was employed as an arm polymer and the α-chloro-α-phenylacetyl group was introduced at the end of the PEO chain (PEO-Cl macroinitiator).[38,40,41] As a result of the above investigation, the Eu-PEO star was prepared by simultaneous introduction (**Scheme 2.2**).

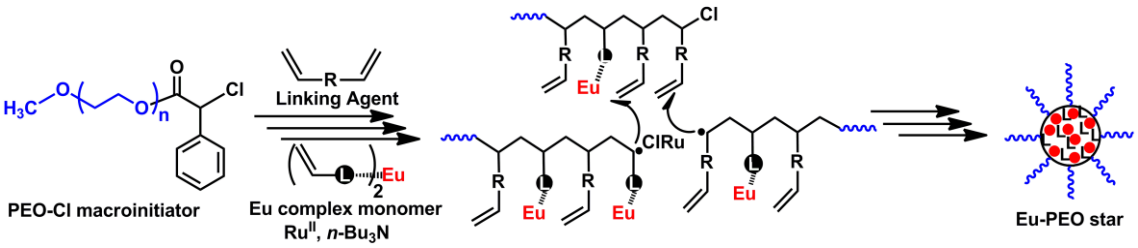

SCHEME 2.2. Synthesis of water-soluble Eu(III)-bearing star polymer.

The star formation proceeded more slowly than in the case of PMMA star formation and the yield of the Eu-PEO star was lower, ca. 55% at 158 h from the GPC curve area (**Fig. 4**). To obtain the water-soluble Eu-PEO star, some adjustments in the concentration ratio of the linking agent EGDMA to PEO-Cl macroinitiator were made. The water-soluble Eu-PEO star was obtained at the ratio of $[EGDMA]_0/[PEO\text{-}Cl]_0$ of 2.5. The core of the star polymer was hydrophobic; however, the water-soluble PEO arms had eliminated the hydrophobic property of the core and water-soluble Eu(III)-bearing star polymer was obtained. The obtained Eu-PEO star was characterized using GPC, resulting in high molecular weight ($M_w \approx 125{,}000$) and relatively narrow MWD ($M_w/M_n \approx 1.58$).

The concentration of Eu(III) ion in the Eu-PEO star was also evaluated to be 33 μmol/g-polymer from its UV absorption spectrum and was in good agreement with that determined from MIP–MS, 39 μmol/g-polymer. The diameter of the Eu-PEO star was

found using DLS to be 18 nm. In contrast, water-insoluble star polymer was formed with higher $[EGDMA]_0/[PEO\text{-}Cl]_0$ ratios (data not shown). If too much hydrophobic EGDMA and Eu(SDPO) were employed, the formed core would be larger and could not be covered with hydrophilic PEO arms, resulting in the water-insoluble polymer.

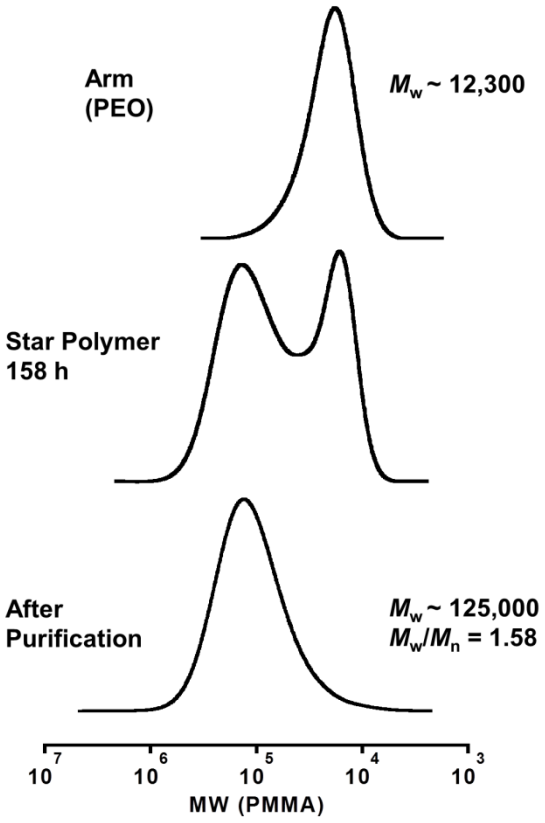

FIGURE 4. MWD curves of Eu-PEO star obtained from PEO arms with EGDMA and Eu(SDPO) in toluene at 80 °C: $[PEO]_0$ = 13.3 mM; $[EGDMA]_0$ = 33.3 mM; $[Eu(SDPO)]_0$ = 33.3 mM; $[Ru(Ind)Cl(PPh_3)_2]_0$ = 1.33 mM; $[n\text{-}Bu_3N]_0$ = 26.6 mM.

Stability of Eu-PEO star in water

The stability of Eu-PEO star in water was examined because the Eu(III) ion has considerable hydrophilic character and ligand exchange between phosphine oxide and water may take place. Eu-PEO star polymer had an identical UV-vis spectrum in water to that in CH_2Cl_2. The absorbance at 305 nm of the aqueous solution of Eu-PEO star was monitored for one month (**Fig. 2.5**). The absorbance decreased in the initial five days but was almost constant after seven days, which implies good stability of Eu-PEO star in water. In contrast, Eu(SDPO) showed slow decomposition in water/MeOH (50/50, v/v), resulting in ca. 25% decrease in absorbance in 30 days. Specifically stabilized coordination chemistry of star polymers in aqueous media has also been reported for Fe-bearing star polymer.[34]

Figure 2.6 also showed the stability of Eu-PEO star in different pH condition. Generally, the cancer cells environment was little bit acidic condition. Eu-PEO star was stable under acidic condition in the range of pH: 5-7. This result suggested that Eu-PEO star would be possible to be used as luminescence probe and X-ray sensitizer within cancer cells.

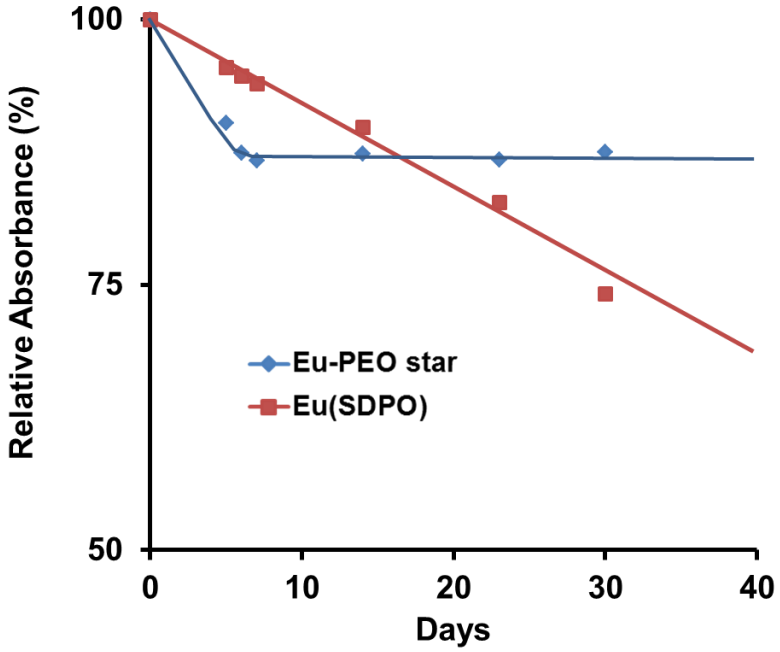

FIGURE 2.5. The stability of Eu-PEO star and Eu(SDPO) in water and mixed water–methanol, respectively.

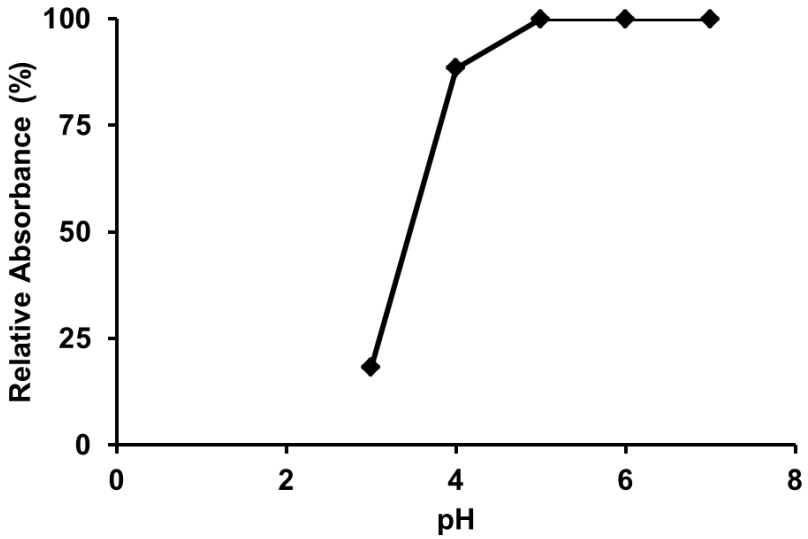

FIGURE 2.6. The stability of Eu-PEO star in different pH condition.

Luminescent photoproperties of Eu(III)-bearing star polymers

Figure 2.7 shows a photograph of the fluorescence of Eu-PMMA star (A) and Eu-PEO star (B) solution with 14 μM of [Eu(III)] in CH_2Cl_2 under 365 nm UV irradiation. Both Eu-bearing star polymers exhibited strong fluorescence and the emission intensity of Eu-PEO star was stronger than that of Eu-PMMA star.

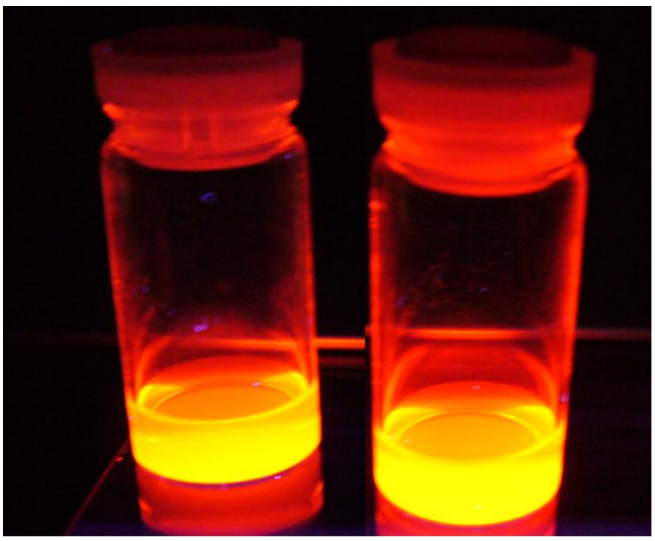

FIGURE 2.7. Eu(III)-PMMA star (a) and Eu(III)-PEO star (b) under 365 nm of UV light irradiation in CH_2Cl_2, [Eu] = 14 μM.

Figure 2.8 presents fluorescence spectra of Eu-PEO star, Eu-PMMA star, and Eu(SDPO) in different solvents. Fluorescence spectra were normalized with respect to

the intensity of the magnetic dipole transition ($^5D_0$–$^7F_1$) at 595 nm, which is known to be less sensitive to the surrounding environment of the Eu(III) ion.[42] In CH_2Cl_2, a good solvent for all of the samples (Eu-PEO star, Eu-PMMA star, and Eu(SDPO)), the fluorescence spectra were almost identical with the three emission bands at 581 nm (electric dipole transition, $^5D_0$–$^7F_0$), 595 nm, and 615 nm (electric dipole transition, $^5D_0$–$^7F_2$). The emission intensity at 615 nm is known to depend markedly on the coordination geometry[42] and the similarities of the spectra of the samples suggest that the coordination geometries around the Eu(III) center of Eu(SDPO) are maintained even in the star polymer with hydrophobic and hydrophilic arms.

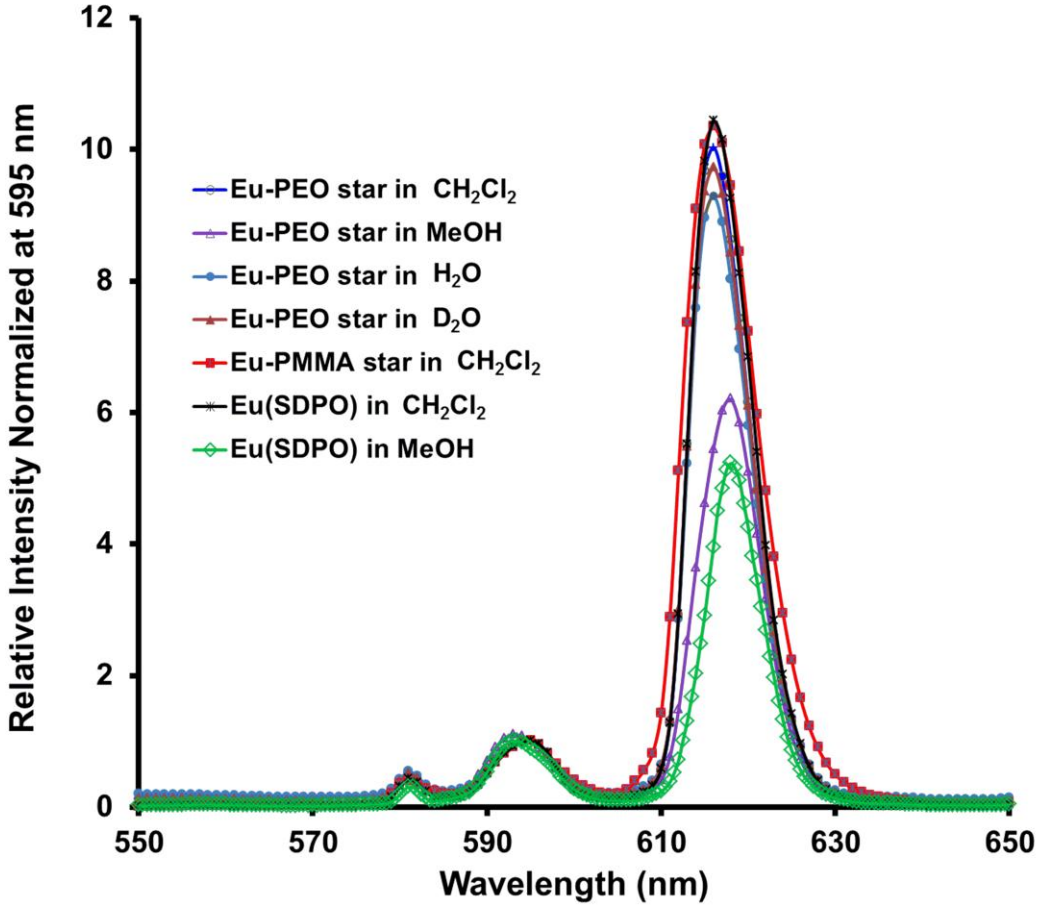

FIGURE 2.8. Fluorescence spectra of Eu-PMMA star, Eu-PEO star, and Eu(SDPO) in different solvents (excitation wavelength: 365 nm).

In both water and deuterated water, the fluorescence spectra of Eu-PEO star were close to that in CH_2Cl_2 with the slight decrease in the relative intensity of the 615 nm band suggesting stability of the coordination geometry around the Eu(III) center against environmental conditions (**Fig. 2.9**). In contrast, the fluorescence spectra of Eu-PEO star and Eu(SDPO) in MeOH were clearly different from those in CH_2Cl_2 and water.

The relative intensities of the emission band of the $^5D_0$–$^7F_2$ electronic dipole transition were much smaller than those in CH_2Cl_2 and water and exhibited a slight red shift of the emission peak to 618 nm. These results indicate that the coordination geometries of Eu-PEO star and Eu(SDPO) in MeOH were different from those in CH_2Cl_2 and water.

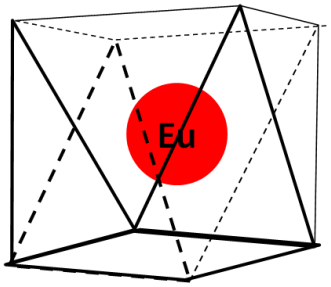

Figure 2.9. Coordination sites of Eu(III) complexes.[35]

The emission lifetimes and quantum yields of Eu-PEO star, Eu-PMMA star, and Eu(SDPO) in different solvents were also measured (**Table 2.2**). In CH_2Cl_2 (entries 1, 5, and 6), a relatively long emission lifetime of about 0.8 ms was observed for all Eu(III) compounds. The quantum yield of Eu-PEO star was quite high (59%), which corresponds to a relatively low nonradiative rate constant (k_{nr}), which was close to those of Eu(SDPO) in various conditions. The quantum yield of Eu-PMMA star was lower (44%) than that of Eu(SDPO) because of a smaller radiative rate constant (k_r). The reason for the difference in quantum yields is not clear; however, the nature of the

surrounding arm polymer might affect k_r, k_{nr}, and the quantum yield.

In MeOH, the quantum yield of Eu-PEO star and Eu(SDPO) (entries 2 and 7, respectively) dramatically decreased and the emission lifetime also decreased to about half of that in CH_2Cl_2, which corresponds to a much higher k_{nr} value in MeOH. Such a significant difference seems to originate from a modification in the coordination geometry in MeOH which the geometry structure became more symmetry and relaxed. Because the core of the star polymer consists of many ester groups, MeOH molecules can enter the core and interact with the Eu complex to change the coordination geometry, resulting in lower $^5D_0$–$^7F_2$ emission and a reduced quantum yield. The nonradiative transitions of lanthanide complexes are affected by the molecular vibrations of C–H and O–H bonds of the solvent.[42,43] Considering the solvation effects, together with increasing abilities of direct coordination of solvent molecules to the Eu(III) center, the solvent molecule motions consumed energy, thus the radiative transition of Eu(III) decreased.[44]

TABLE 2.2 Emission lifetimes and quantum yields of Eu(III)-star polymer and Eu(III)-monomer in different solvents

Entry	Sample	Solvent	Lifetime (τ, ms)[a]	Quantum yield (Φ, %)	$k_r(s^{-1})$[b]	$k_{nr}(s^{-1})$[c]
1	Eu-PEO star	CH_2Cl_2	0.83	59	7.1×10^2	4.9×10^2
2	Eu-PEO star	MeOH	0.32	4	1.3×10^2	30.0×10^2
3	Eu-PEO star	H_2O	0.76	19	2.5×10^2	10.6×10^2
4	Eu-PEO star	D_2O	0.90	19	2.1×10^2	9.0×10^2
5	Eu-PMMA star	CH_2Cl_2	0.83	44	5.3×10^2	6.7×10^2
6	Eu(SDPO)	CH_2Cl_2	0.75	69	9.2×10^2	4.1×10^2
7	Eu(SDPO)	MeOH	0.42	10	2.4×10^2	21.0×10^2

[a] Emission lifetime of the Eu(III) complexes were measured by excitation at 365 nm.

[b] Radiative rate constants $k_r = \Phi/\tau$ observed.

[c] Nonradiative rate constants $k_{nr} = 1/\tau - k_r$.

The quantum yield of Eu-bearing PEO star in water was about 20% (entry 3) and is higher than some previous Eu-based fluorescence dyes such as [4′-(10-methyl-9-anthryl)-2,2′:6′,2″-terpyridine-6,6″-diyl]bis(methylenenitrilo)tetrakis(acetate)-Eu(III), which has been reported to show a quantum yield of 0.9%.[24] A

water-soluble Eu(III) complex with modified pybox ligand exhibited a high quantum yield in H_2O, 30%;[45] however, it required much more complicated synthetic chemistry than that of the present Eu-PEO star.

The fluorescence spectrum and the emission lifetime of Eu-PEO star in water were very close to those in CH_2Cl_2. The luminescence property of Eu-PEO star in deuterated water was also examined because it has been reported that the introduction of deuterium in hexafluoro-2,4-pentanedione (hfa-H_2) ligand of Eu(III) ion can easily occur from a deuterated protic solvent and enhances the emission quantum yield of the Eu(III) complex.[35,36,42] Interestingly, the quantum yield and other parameters of Eu-PEO star were not influenced by D_2O, which suggests that hydrogen–deuterium exchange between the hfa-H_2 ligand and D_2O did not occur. These results thus indicate that the nature of the core in PEO-star is sufficiently hydrophobic to prevent water molecules access to the core even though Eu-PEO star is soluble in water, which is beneficial for the specific stability of the Eu(III) coordination structure in water.

2.4. CONCLUSIONS

In this chapter, I have demonstrated the syntheses of Eu(III)-bearing star polymer using PMMA and PEO as an arm of the each star polymer. One step introduction by living radical copolymerization of Eu(III)-bearing monomer [Eu(SDPO)] and divinyl linking monomer (EGDMA) proved to be simple and effective method. Water soluble Eu(III)-bearing star polymer was obtained by using PEO as an arm. The obtained Eu(III)-bearing star polymers have luminescence properties with relatively high quantum yield even in water. This water soluble Eu(III)-bearing star polymer is promising candidate for biological applications such as bioimaging and X-ray sensitizer for detecting and curing tumor, respectively.

2.5. REFERENCES

1. You, Z.; Bi, X.; Fan, X.; Wang, Y. *Acta Biomater.* **2012**, *8*, 502–510.

2. Schulz, D. N.; Patil, A. O. In Functional Polymers: An Overview, Functional Polymers, ACS Symposium Series 704; American Chemical Society: Washington, DC, 1998; pp. 1–14.

3. Gauthier, M. A.; Gibson, M. I.; Klok, H. A. *Angew. Chem., Int. Ed*. **2009**, *48*, 48–58.

4. Suzuki, Y.; Makino, Y. *J. Controlled Release* **1999**, *62*, 101–107.

5. Jagur-Grodzinski, J. *React. Func. Polym.* **1999**, *39*, 99–138.

6. Wu, W. C.; Chen, C. Y.; Tian, Y.; Jang, S. H.; Hong, Y.; Liu, Y.; Hu, R.; Tang, B. Z.; Lee, Y. T.; Chen, C. T.; Chen, W.-C.; Jen A. K. Y. *Adv. Funct. Mater.* **2010**, *20*, 1413–1423.

7. Koide, Y.; Urano, Y.; Hanaoka, K.; Terai, T.; Nagano, T. *J. Am. Chem. Soc.* **2011**, *133*, 5680–5682.

8. Zhang, Y.; Yang, J. *J. Mater. Chem. B* **2013**, *1*, 132–148.

9. Yordanov, G.; Bedzhova, Z. *Eur. J. Chem.* **2011**, *9*, 1062–1070.

10. Lu, Z. Y.; Yuan, T. S.; Chen, Y. L.; Wei, X. Q.; Zhu, W. G.; Xie, M. G. *Chinese Chem. Lett.* **2002**, *13*, 674–677.

11. Trenor, S. R.; Shultz, A. R.; Love, B. J.; Long, T. E. *Chem. Rev.* **2004**, *104*, 3059–3077.

12. Auger, A.; Samuel, J.; Poncelet, O.; Raccurt, O. *Nanoscale Res. Lett.* **2011**, *6*, 328:1–6.

13. Chen, F.; Huang, P.; Zhu, Y. J.; Wu, J.; Cui, D. X. *Biomaterials* **2012**, *33*, 6447–6455.

14. Chen, F.; Zhu, Y. J.; Zhang, K. H.; Wu, J.; Wang, K. W.; Tang, Q. L.; Mo, X. M. *Nanoscale Res. Lett.* **2011**, *6*, 67:1-9.

15. Yang, P. P.; Quan, Z. W.; Li, C. X.; Kang, X. J.; Lian, H. Z.; Lin, J. *Biomaterials* **2008**, *29*, 4341–4347.

16. Bunzli, J. C. G. *Chem. Rev*. **2010**, *110*, 2729–2755.

17. Feng, J.; Shan, G.; Maquieira, A.; Koivunen, M. E.; Guo, B.; Hammock, B. D.; Kennedy, I. M. *Anal. Chem*. **2003**, *75*, 5282–5286.

18. Davies, A.; Lewis, D. J.; Watson, S. P.; Thomas, S. G.; Pikramenou, Z. *Proc. Natl. Acad. Sci. U.S.A.* **2012**, *109*, 1862–1867.

19. Chen, Y.; Lu, Z. *Anal. Chim. Acta* **2007**, *587*, 180–186.

20. Sculimbrene, B. R.; Imperiali, B. *J. Am. Chem. Soc.* **2006**, *128*, 7346–7352.

21. Zhao, Y.; Gao, J. *Chem. Commun.* **2012**, *48*, 2997–2999.

22. Cable, M. L.; Kirby, J. P.; Sorasaenee, K.; Gray, H. B.; Ponce, A. *J. Am. Chem. Soc.* **2007**, *129*, 1474–1475.

23. Song, B.; Wang, G.; Tan, M.; Yuan, J. *J. Am. Chem. Soc.* **2006**, *128*, 13442–13450.

24. Bruce, J. I.; Dickins, R. S.; Govenlock, L. J.; Gunnlaugsson, T.; Lopinski, S.; Lowe, M. P.; Parker, D.; Peacock, R. D.; Perry, J. J. B.; Aime, S.; Botta, M. *J. Am. Chem. Soc.* **2000**, *122*, 9674–9684.

25. Mathis, G. *Clin. Chem.* **1993**, *39*, 1953–1959.

26. Xi, P.; Cheng, K.; Sun, X.; Zeng, Z.; Sun, S. *Chem. Commun*. **2012**, *48*, 2952–2954.

27. Picot, A.; D'Aléo, A.; Baldeck, P. L.; Grichine, A.; Duperray, A.; Andraud, C.; Maury, O. *J. Am. Chem. Soc.* **2008**, *130*, 1532–1533.

28. Grubbs, R. B. *J. Polym. Sci. Part A: Polym. Chem.* **2005**, *43*, 4323–4336.

29. Hardy, C. G.; Ren, L. X.; Tamboue, T. C.; Tang, C. B. *J. Polym. Sci. Part A: Polym. Chem.* **2011**, *49*, 1409–1420.

30. Terashima, T.; Kamigaito, M.; Baek, K.-Y.; Ando, T.; Sawamoto, M. *J. Am. Chem. Soc.* **2003**, *125*, 5288–5289.

31. Gao, H.; Matyjaszewski, K. *Prog. Polym. Sci*. **2009**, *34*, 317–350.

32. Terashima, T.; Ouchi, M.; Ando, T.; Kamigaito, M.; Sawamoto, M. *J. Polym. Sci. Part A: Polym. Chem*. **2006**, *44*, 4966–4980.

33. Terashima, T.; Ouchi, M.; Ando, T.; Kamigaito, M.; Sawamoto, M. *Macromolecules* **2007**, *40*, 3581–3588.

34. Terashima, T.; Nomura, A.; Ito, M.; Ouchi, M.; Sawamoto, M. *Angew. Chem., Int. Ed.* **2011**, *50*, 7892–7895.

35. Hasegawa, Y.; Yamamuro, M.; Wada, Y.; Kanehisa, N.; Kai, Y.; Yanagida, S. *J. Phys. Chem. A* **2003**, *107*, 1697–1702.

36. Hasegawa, Y.; Sogabe, K.; Wada, Y.; Kitamura, T.; Nakashima, N.; Yanagida, S. *Chem. Lett.* **1999**, *28*, 35–36.

37. Jiang, J.; Tong, X.; Zhao, Y. *J. Am. Chem. Soc*. **2005**, *127*, 8290–8291.

38. Li, W.; Matyjaszewski, K. *J. Am. Chem. Soc.* **2009**, *131*, 10378–10379.

39. Sanmartin, J.; Bermejo, M. R.; Sousa, A.; Fondo, M.; Gomez-Forneas, E.; McAuliffe, C. *Acta Chem. Scand*. **1997**, *51*, 59–68.

40. Baek, K. Y.; Kamigaito, M.; Sawamoto, M. *Macromolecules* **2001**, *34*, 7629–7635.

41. Vidts, K. R. M.; Du Prez, F. E. *Eur. Polym. J.* **2006**, *42*, 43–50.

42. Miyata, K.; Nakanishi, T.; Fushimi, K.; Hasegawa, Y. *J. Photochem. Photobiol., A* **2012**, *235*, 35–39.

43. Kawa, M.; Fréchet, J. M. J. *Chem. Mater.* **1998**, *10*, 286–296.

44. Lei, K. W.; Liu, W. S.; Tan, M. Y. *Spectrochim. Acta, Part A* **2007**, *66*, 590–593.

Chapter 3

X-ray Sensitizing Effect of Eu(III)-bearing Star Polymer

3.1. Introduction

Radiation therapy or radiotherapy which is used for cancer therapy has the advantage of noninvasiveness compare to surgical treatment. Typical dose of X-ray in radiotherapy for a tumor ranges from 60 to 80 Gy in ca. 2 Gy fractions that are almost near lethal dose of the cells. High irradiation dose may induce various side effects, such as inflammation of tissues and organs in and around the body site radiated. To overcome those problems, specific material (X-ray sensitizer) that enhances the X-ray absorption could be used. Hence, the low irradiation dose could be applied to treat cancer. Metal atoms are chosen as candidates of X-ray sensitizer because the absorption efficiency increases roughly in proportion to Z^4-Z^5 (Z is atomic number). Heavy metals are thought to be good X-ray sensitizer but their ions also have serious toxicity. In this work, star polymer is employed to suppress the toxicity by holding the metal ion in the core of star polymer. The purpose of this research is to develop Eu(III)-bearing star polymer as X-ray sensitizer materials.

It has been known that the dose was increased when a high-Z material was in the targeted area.[1] As far as I know, the earliest biological report appeared more than 30 years ago when chromosomal damage was noticed in circulating lymphocytes from patients undergoing iodine contrast angiography.[2] Other early reports were a study of the cytogenetic effects of contrast media,[3] and measurements in patients of the increased dose during iodine contrast angiography.[4] In an in vitro experiment more than 25 years ago, iodine contrast medium was found to radiosensitize cells.[5] To make use of the Auger electrons and the photoelectric effect, iododeoxyuridine (IUdR) was incorporated into cellular DNA in vitro,[6] yielding a radiotherapeutic advantage of ~3, as

suggested earlier.[7] Theoretical and experimental studies of high-Z dose enhancement over both the megavolt and orthovoltage range have been reported.[8,9] Regulla et al (1998, 2002) grew cells on a gold foil that was irradiated (40–120 kVp) and measured a dose enhancement factor (DEF)[10,11] of more than 100, with secondary electrons travelling over a range of up to 10 mm. Herold et al. in 2000 injected 1.5–3.0 mm gold particles directly into a tumour followed by irradiation.[12] Santos Mello et al. in 1983 directly injected tumours with iodine contrast media followed by 100-kVp X-rays and obtained remission in 80% of radioresistant tumours in mice.[11] Norman et al. in 1997 modified a computed tomography (CT) scanner by inserting a collimator to narrow the beam in both directions to encompass the tumour only (and not the entire subject).[12]

When X-rays impinge on matter, a number of processes can result (**Figure 3.1**.).[13] The emissions relevant are scattered photons (X-rays), photoelectrons, Compton electrons, Auger electrons and fluorescence photons. When an incident photon ejects an electron from an inner shell of an atom, this photoelectron acquires a kinetic energy of the primary beam minus its binding energy, and this kinetic energy determines the range it will have in the tissue, which can be for example 100 μm or about 10 cell diameters for an electron of about 100 keV energy. This photoelectric effect varies approximately as $(Z/E)^3$, where E is the incident photon energy and Z is the atomic number of the target. For high-Z elements it dominates the interaction with matter at energies <0.5 MeV.

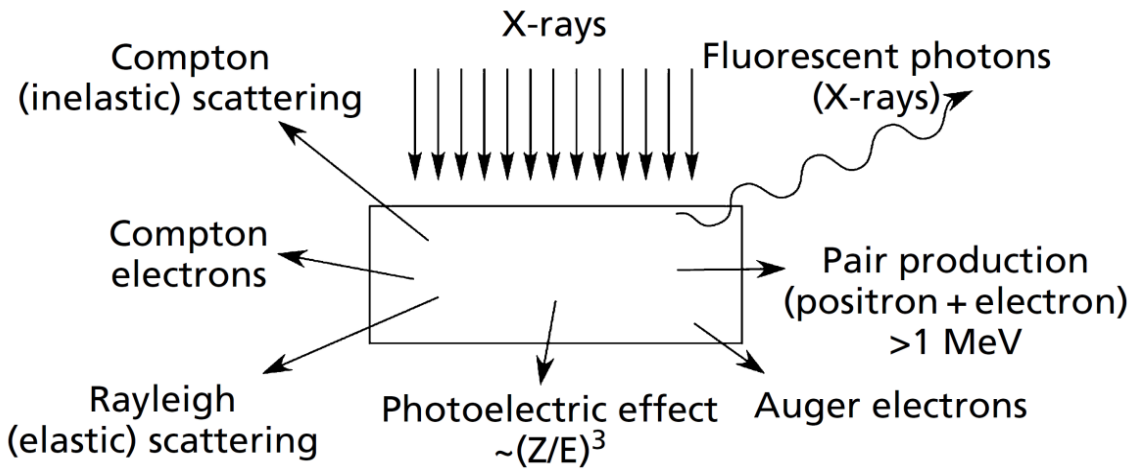

Figure 3.1. Interaction of X-ray with matter

In this chapter, the effect of Eu(III)-bearing star polymer as X-ray sensitizer was investigated by employing plasmid DNA. The advantages of Eu(III) in this research was to increase the dose absorption and also might be used as bioimaging materials because of the photoproperties of Eu(III).

3.2. Experimental

3.2.1. Materials

Water-soluble Eu(III)-bearing star polymer was obtained from the synthesis of Eu(III)-PEO star polymers on Chapter 2. Plasmid DNA pEGFP-N1 was amplified in E. coli and purified using a Plasmid Mega Kit (Qiagen) according to the manufacturer's instructions. The purity and concentration of the plasmid DNA were determined by UVevis spectrometry and agarose gel electrophoresis. Ultrapure agarose and SYBR®Gold nucleic acid gel stain was obtained from Invitrogen and used as received .

3.2.2. Instruments

X-ray irradiation was done by using Faxitron CP-160 X-ray irradiation system. The image of gel electrophoresis was scanned and quantified by densitometry with an ImageMaster VDS-CL camera (Amersham Biosciences, Buckinghamshire, UK).

3.2.3. X-ray irradiation Effect

Plasmid DNA, pEGFP-N1[14] in TE buffer, was mixed with Eu(III)-bearing star polymer therefore the concentration of Eu(III)-bearing star polymer in solutions were 1, 2, 5 and 10 μM with 20 ng/mL pEGFP-N1 concentration respectively. The solutions were placed on 96-well plates and then irradiated by X-ray in the chamber of Faxitron X-ray machine unit with doses as: 1 Gy (75 kVp, 2.1 minutes) and 5 Gy (75 kVp, 10.6 minutes). For the control, 5 samples with various Eu(III)-bearing star polymer

concentrations were kept in dark room. Four repeating experiments were done to observe the sensitizing effect.

3.2.4. Agarose gel electrophoresis

After irradiation, the 96-well plates was removed from the Faxitron X-ray machine chamber and immediately 1 µL from each solutions were taken and mixed with 9 µL of loading buffer. The different forms of stranded plasmid DNA were separated by 0.8% of agarose gel electrophoresis in TAE buffer (40 m*M* Tris-acetate, 1 m*M* EDTA, pH 8.0). Each sample solution was then loaded into the agarose gel wells and run for 30 min at 100 volt. After the electrophoresis, the gel was stained with SYBR Gold (diluted 10,000 times with TAE buffer for 30 min.). In the analysis, Eu(III)-bearing star polymers were found to have negligible effects on the migration of DNA in electrophoresis.

3.3. Result and Discussion:

3.3.1. DNA Damage by Eu(III)-bearing Star Polymer: various sensitizer concentration irradiation doses)

To observe the effect of Eu(III)-bearing star polymer as X-ray sensitizer (radiosensitizer), plasmid DNA (pEGFP-N1) was employed. Eu(III)-bearing star polymer was mixed with pEGFP N-1 in different concentration and irradiated by X-ray in various doses. Agarose gel electrophoresis was used to determine the DNA strand breaks in pEGFP-N1 after the irradiation in the presence of Eu(III)-bearing star polymer (**Figure 3.2**). In this discussion, the effect of Eu(III)-bearing star to the pEGFP-N1 under X-ray irradiation was defined as dose enhancement. Heavy metal was supposed to increase the absorption of X-ray irradiation therefore dose enhancement was defined to determine the work of Eu(III)-bearing star polymer as radiosensitizer. In this research, dose enhancement was determined as the ratio of DNA strand breaks with and without Eu-star polymer under X-ray irradiation (eq. 3.1).

$$dose\ enhancement = \frac{A - A'}{B - B'} \qquad \text{eq. 3.1}$$

A': sample with Eu(III) in certain radiation dose
A: sample with Eu(III) in 0 Gy dose
B': sample without Eu(III) in certain radiation dose
B : sample without Eu(III) in 0 Gy dose

Eu(III)-bearing star polymer with 1, 2, 5 and 10 μM concentration was mixed with 20 ng/mL pEGFP-N1 and then irradiated with 1 Gy and 5 Gy dose of X-ray irradiation. In the agarose gel electrophoresis, the pEGFP-N1 would show two bands:

open circular and supercoiled DNA. The single strand break DNA basically could be observed if the amount of open circular DNA was increased which comes from the breaking of supercoiled DNA. The double strand breaks DNA would be observed if the linear DNA band was appeared. From **Figure 3.2.,** the effect of Eu(III)-bearing star polymer was observed qualitatively in compare to the sample without Eu(III)-bearing star polymer. From the agarose gel electrophoresis, the intensity of pEGFP-N1 was relatively decreased by increasing the concentration and X-ray irradiation doses. Eu(III)-bearing star polymer in 10 μM concentration under 5 Gy X-ray irradiation dose showed relatively lesser intensity than that of without Eu(III)-bearing star polymer. Generally, by increasing the Eu(III)-bearing star polymer and increasing of X-ray irradiation dose, the intensity of DNA bands in agarose gel electrophoresis was decreased which suggested the effectiveness of Eu(III)-bearing star polymer as X-ray sensitizer. Schematically the breaking or degradation of plasmid DNA was shown in **Figure 3.3**. Plasmid DNA, pEGFP-N1, contained supercoiled and open circular DNA therefore under X-ray irradiation, if single strand break was occurred, generally the amount of open circular DNA would increased by decreasing the number of supercoiled DNA. Furthermore, if double strand breaks DNA was occurred, the amount of open circular and supercoiled DNA would decrease.

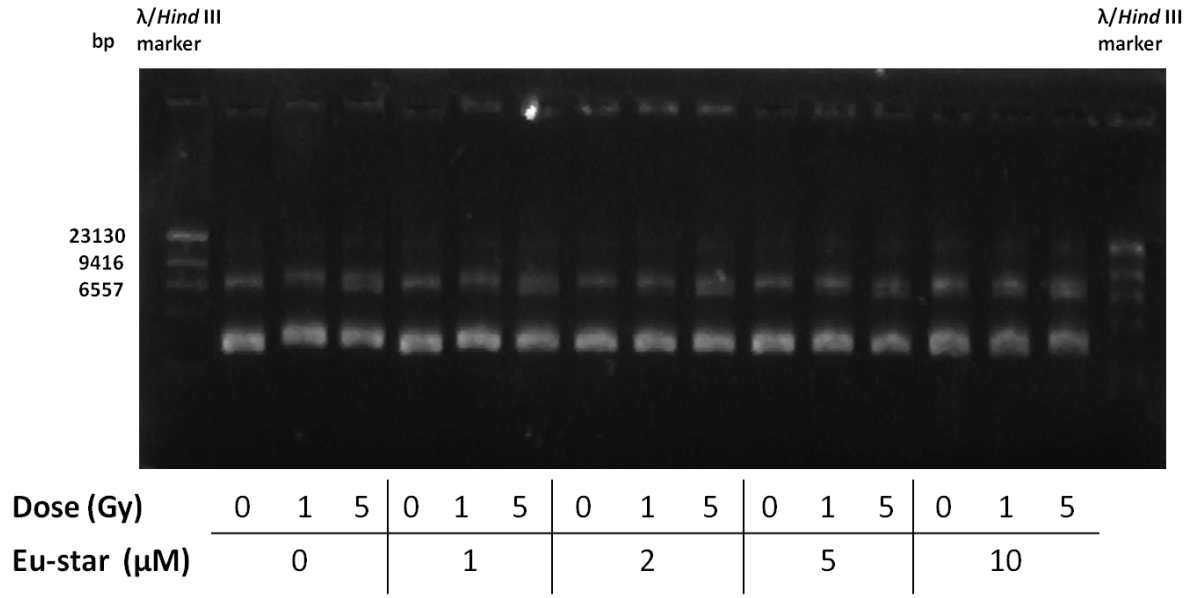

Figure 3.2. Agarose gel electrophoresis image after staining with SYBR gold for 30 min.

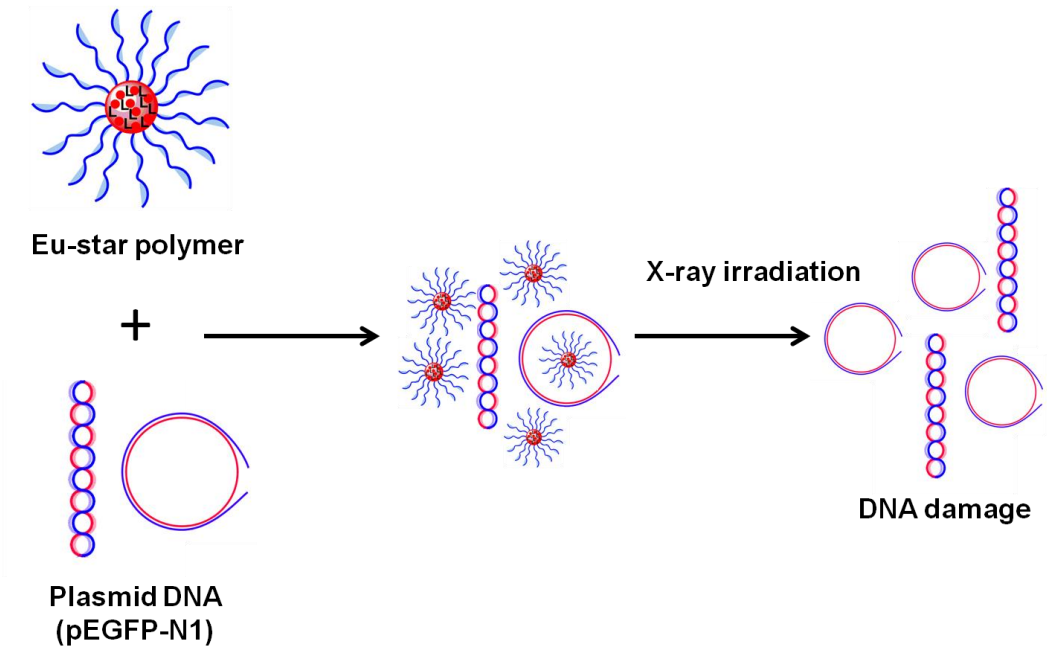

Figure 3.3. DNA breaking or degradation under X-ray irradiation in the presence Eu(III)-star polymers.

Figure 3.4 showed the quantitative data of Eu(III)-bearing star polymer effects. Eu(III)-bearing star polymer with 10 µM concentration under 5 Gy X-ray irradiation dose showed the high dose enhancement effect, almost twice of the sample without Eu(III)-bearing star polymers. In the other hand, the Eu(III)-bearing star polymer with 5 µM concentration under 1 Gy X-ray irradiation dose showed about 1.5 times dose enhancement. Interestingly, even in 1 µM concentration, the dose enhancement still could be observed even it was not as significant as 5 µM concentration.

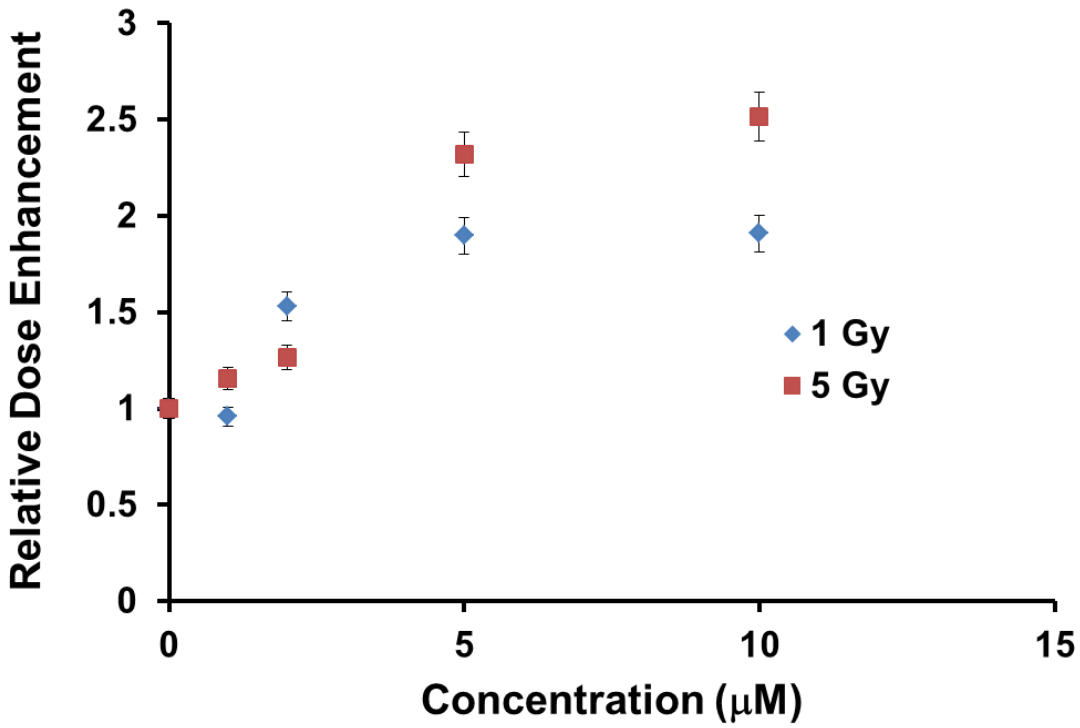

Figure 3.4. Dose enhancement of X-ray in the presence Eu(III)-bearing star polymers.

From those result, the dose enhancement was predicted from the absorption of X-ray by Eu(III) metal and several interaction between the Eu(III) and X-ray might be

occurred. Generally, the photoelectric effect and auger electron were supposed to be responsible to the dose enhancement effects. As describe in Chapter 1, it had been known that the radicals which come from the reaction of electron and water (ionizing water) could be destructing the DNA strands. However, at present, it is still difficult to show which interaction that effective to increase the electron and eventually increase the DNA strand breaks. The amount of DNA under X-ray irradiation in the presence of Eu(III)^star polymers also observed here as shown in **Figure 3.5.** In general, the amount of DNA was decreased by increasing the dose and concentration of Eu(III)-bearing star polymers even though in the condition without X-ray irradiation the amount of DNA was decreased which could be resulted from the environment. The presence of oxygen and preparation under normal room light may responsible to generate singlet oxygen that caused DNA degradation. Under room light and in the presence of oxygen, the energy transfer between Eu(III) ion to oxygen could take place producing singlet oxygen (photosensitizer). This singlet oxygen was supposed to be responsible to DNA degradation. However it is still unclear to present in detail, the mechanism of DNA degradation in the presence of Eu(III) ion without X-ray irradiation.

Recently, research in X-ray sensitizer was done for gold nanoparticles, however it is also still unclear about the interaction mechanism between the X-ray and gold nanoparticles to enhance the DNA strand breaks. The dose enhancement of gold nanoparticle as X-ray sensitizer was 2 times in 1% weight gold nanoparticle concentration which is relatively small to that of Eu(III)-bearing star polymers in the same concentration.

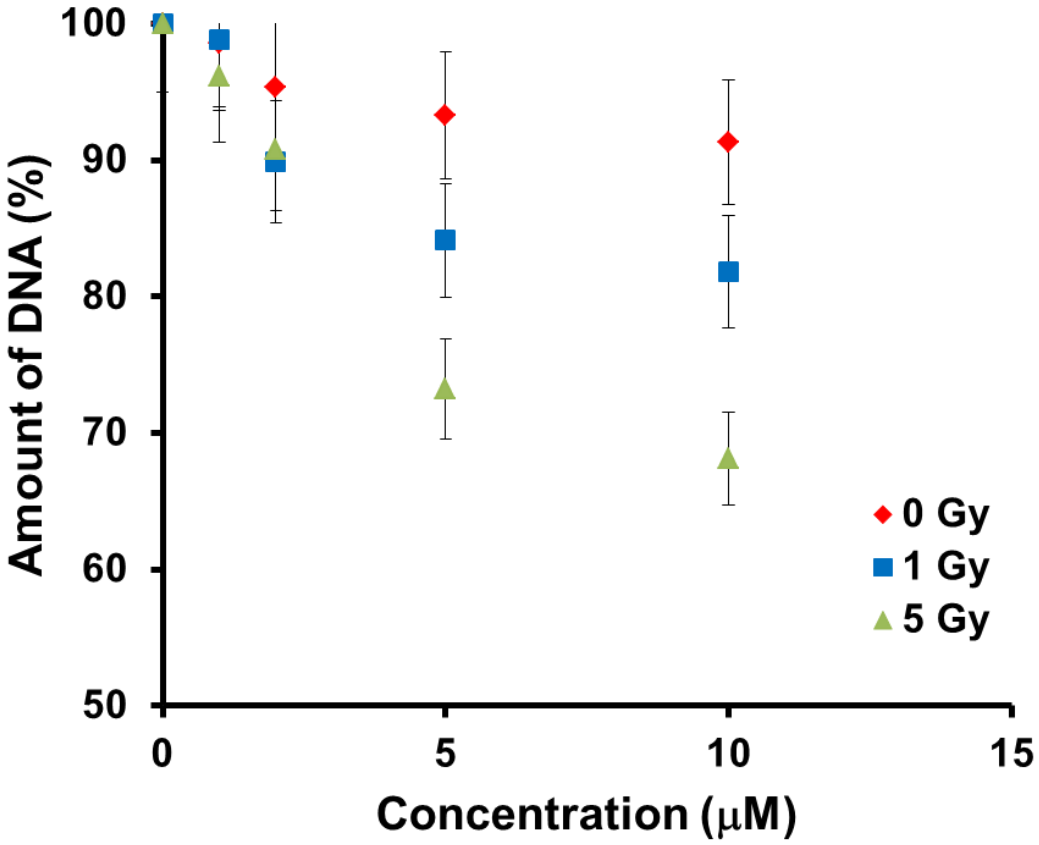

Figure 3.5. DNA degradation under X-ray irradiation in the presence of Eu(III)-bearing star polymers.

3.4. Conclusion

Eu(III)-bearing star polymer is giving new breakthrough as new X-ray sensitizer. The observation by employing plasmid DNA under X-ray irradiation is promising to be utilized as X-ray sensitizer. The luminescence properties of Eu(III)-bearing star polymer are also promising to be used as bioimaging. Therefore, Eu(III)-bearing star polymer could be used not only for curing the cancer cells but also to imaging the cancer tissues.

3.5. References

1. Spiers, F. W. *Br. J. Radiol*. **1949**, 22, 521–533.

2. Adams, F. H.; Norman, A.; Mello, R. S.; Bass, D. *Radiology* **1977,** *124*, 823–826.

3. Norman, A.; Adams, F. H., Riley, R. F. *Radiology* **1978**, *129*, 199–203.

4. Callisen, H. H.; Norman, A.; Adams, F. H. *Med. Phys*. **1979**, *6*, 504–509.

5. Matsudaira, H.; Ueno, A. M.; Furuno, I. *Radiat. Res*. **1980**, *84*, 144–148.

6. Nath, R.; Bongiorni, P.; Rockwell, S. *Radiat. Res*. **1990**, *124*, 249–258.

7. Fairchild, R. G.; Brill, A. B.; Ettinger, K. V. *Invest. Radiol*. **1982**, *17*, 407–416.

8. Das, I. J.; Kahn, F. M. *Med.Phys*. **1989**, *16*, 367–375.

9. Das, I. J.; Chopra, K. L. *Med. Phys*. **1995**, *22*, 767–773.

10. Regulla, D. F.; Hieber, L. B.; Seidenbusch, M. *Radiat. Res*. **1998**, *150*, 92–100.

11. Regulla, D.; Schmid, E.; Friedland, W.; Panzer, W.; Heinzmann, U.; Harder, D. *Radiat. Res*. **2002**, *158*, 505–515.

12. Herold, D. M.; Das, I. J.; Stobbe, C. C.; Iyer, R. V.; Chapman, J. D. *Int. J. Radiat. Biol*. **2000**, *76*,1357–1364.

13. Hainfeld, JF; Dilmanian, A; Slatkin DN and Smilowitz, HM. *J. Pharm. Pharmacol*. **2008**, *60*, 977-985.

14. Obata, M.; Kobori, T.; Hirohara, S.; Tanihara, M. *Polymer* **2012**, *53*, 4672-4677.

Chapter 4

General Conclusion and Future Outlook

In this thesis, the synthesis of Eu(III)-bearing star polymer and one of its applications was explained. In chapter 1, the general introduction was presented to understand the general views of chapter 2 and 3. Chapter 2 was described the synthesis of Eu(III)-bearing star polymer: first the model synthesis to obtain high Eu(III) introduction and second the synthesis of water-soluble Eu(III)-bearing star polymer. The best introduction of Eu(III) into the star polymer was achieved by using simultaneous procedure. The photoproperties of Eu(III)-bearing star polymer was also discussed in chapter 2 showing relatively high quantum yield and long emission lifetime of water-soluble Eu(III)-bearing star polymer.

In chapter 3, one of the applications of Eu(III)-bearing star polymer was mentioned which applied as the X-ray sensitizer. Eu(III)-bearing star polymer mixing with plasmid DNA, pEGFP-N1, was irradiated with various X-ray dose resulted increasing of DNA strand break. The effect of Eu(III)-bearing star polymer as X-ray sensitizer was quantified as dose enhancement showing two times dose enhancement of X-ray compare to that plasmid DNA without Eu(III)-bearing star polymer. Those suggested that Eu(III)-bearing star polymers are promising as X-ray sensitizer, even though the toxicity and cell uptake should be considered.

From those conclusion in chapter 2 and 3, I could combine the utility of Eu(III)-bearing star polymer to detect (bioimaging probes) and cure the cancer tissues. In other word, in future Eu(III)-star polymer was promising not only for curing the cancer but also for detecting the cancer in the body.

List of Publication and Presentation

Publication:

1. Ahmad Kusumaatmaja, Tsuyoshi Ando, Kayo Terada, Shiho Hirohara, Takuya Nakashima, Tsuyoshi Kawai, Takaya Terashima and Masao Tanihara, Synthesis and Photoproperties of Eu-Bearing Star Polymers as Luminescent Materials and Their Photoproperties, *J. Polym. Sci. Part A: Polym. Chem*. **2013**, accepted.

Presentation:

1. Ahmad Kusumaatmaja, Kayo Terada, Shiho Hirohara, Tsuyoshi Ando and Masao Tanihara, Eu-bearing Star Polymers: Syntheses by Living Radical Polymerization and Their Photoproperties, *61st SPSJ Annual Meeting, Yokohama, Japan*, May 29-31 2012, 61 (1), 3K18.

2. Ahmad Kusumaatmaja, Kayo Terada, Shiho Hirohara, Tsuyoshi Ando and Masao Tanihara, Preparation of Eu-bearing Star Polymers and Their Potential Fluorescence Properties, ACS Fall Meeting 2012, Pensylvania, USA (presented on August 2012).

Acknowledgement

This thesis presents the studies that the author carried out at the Graduate School of Materials Science, during the years from 2010 to 2013 under the supervision of Professor Masao Tanihara and Prof. Tsuyoshi Ando.

The author would like to express his sincerest gratitude to Professor Masao Tanihara and Prof. Tsuyoshi Ando for his continuous guidance, valuable suggestions, and encouragement throughout the present study. The author is also grateful to Professor Kayo Terada, Professor Mime Kobayashi, and Professor Shiho Hirohara (Department of Chemical and Biological Engineering, Ube National College of Technology) for their helpful suggestions.

The author would like to thank Professor Tsuyoshi Kawai for his support to use his equipment and also his helful suggestion. The author would also like to thank Professor Hisao Yanagi for their helpful suggestion in this work. The author would also like to thank Professor Takuya Nakashima and Professor Takaya Terashima (Department of Polymer Chemistry, Graduate School of Engineering, Kyoto University) for their fruitful and helpful discussion.

The author wishes to express his gratitude to Professor Mitsuo Sawamoto (Department of Polymer Chemistry, Graduate School of Engineering, Kyoto University) for the help to facilitate in using his instrument.

Sincere thanks are due to all colleagues in the Biocompatible Materials Science Laboratory for their discussion. The author is also grateful to the support of Graduate School of Materials Science that give me an opportunity to be Research Assistant (RA) for 3 years.

Finally, the author would like to give his greatest thanks to his family, especially his parents, Mr. Suparwoto and Mrs. Murni Kusumandari, his parents in law, Mr. Solekhan and Mrs. Suratinem, his lovely wife Mrs. Ari Dwi Nugraheni, his children, Rayhan Faqih Ahmad and Ghafira Nadira Ahmad, and his brothers Muhammad Iqbal Taftazani and Muhammad Adib Ridhani for their constant assistance and kind-hearted encouragement.

Ahmad Kusumaatmaja

February 2013